

TEXT AND REFERENCES ACCOMPANYING NEVADA BUREAU OF MINES AND GEOLOGY OPEN FILE REPORT 2025-07

Geologic Map of the Arizona Spring Quadrangle, Elko County, Nevada

by

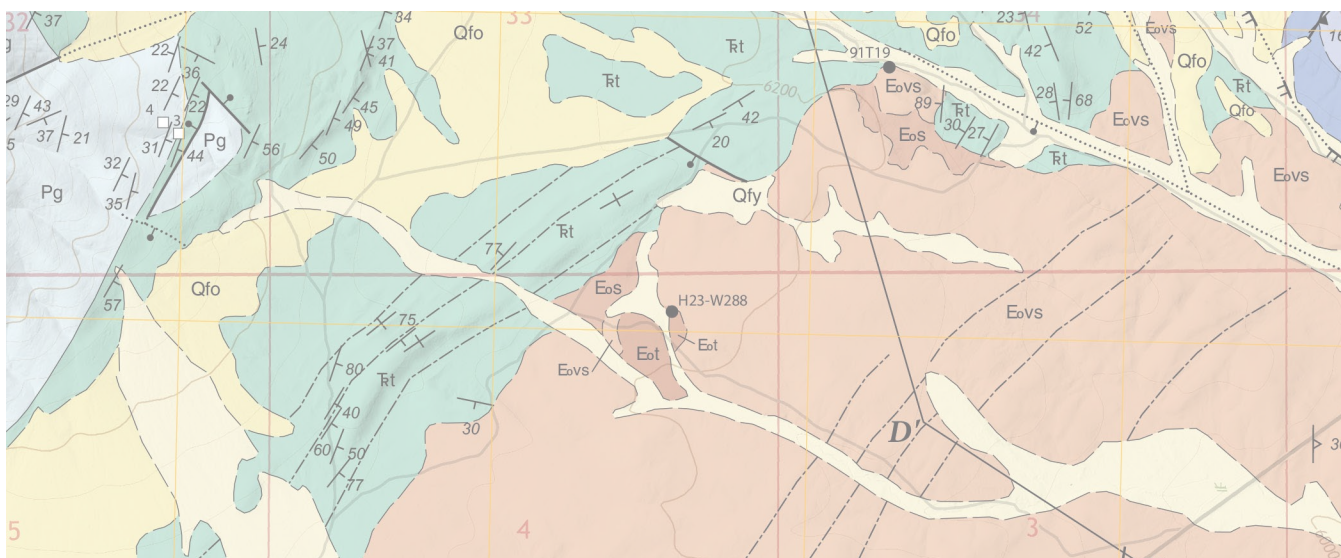
G. Kendall Taylor¹, Arthur W. Snoke², Seth Dee³, Keith A. Howard¹, and Charles H. Thorman¹

¹ Independent Geologist

² University of Wyoming, Laramie, WY

³ Nevada Bureau of Mines and Geology, University of Nevada, Reno

2025



© Copyright 2025 The University of Nevada, Reno. All Rights Reserved.

Suggested citation:

Taylor, G.K., Snoke A.W., Dee, S., Howard, K.A., and Thorman, C., 2025, Geologic map of the Arizona Spring quadrangle, Elko County, Nevada: Nevada Bureau of Mines and Geology Open-File Report 2025-07, scale 1:24,000, 26 p.

NBMG open-file reports have not been formally peer reviewed. This geologic map was funded in part by the USGS National Cooperative Geologic Mapping Program under STATEMAP award number G22AC00578, 2022 and with support from the Geological Society of Nevada.

ABSTRACT

The Arizona Spring quadrangle is located in northeastern Nevada at southeastern end of the East Humboldt Range. The Paleozoic–early Mesozoic rock sequence in the quadrangle can be divided into two distinct structural and metamorphic domains separated by the southeastern East Humboldt detachment fault. Domain 1 consists of a metasedimentary sequence that ranges in protolith age from Cambrian–Ordovician to Devonian–Mississippian. The mapped units in this metamorphic sequence are: Cambrian–Ordovician marble of Verdi Peak, metamorphosed Ordovician Eureka Quartzite, Ordovician–Devonian metadolomite, metamorphosed Guilmette Formation, and Upper Devonian–Mississippian metamorphosed Pilot Shale. These metamorphic rocks have undergone polyphase deformation under amphibolite to greenschist facies conditions. The highest-grade unit is the marble of Verdi Peak, which includes calc-silicate paragneiss that contains tremolite, scapolite, phlogopitic biotite, and scarce diopside. This metamorphic assemblage is the basis of amphibolite facies in domain 1. The lowest grade unit in the metamorphic sequence of domain 1 is the greenschist-facies phyllite of the metamorphosed Pilot Shale. Metamorphosed Guilmette Formation yielded conodonts with a CAI (conodont alteration index) of 5, indicating that this marble reached a temperature of ~300°C. The deformation and metamorphism of the metasedimentary rocks of domain 1 are inferred to be Cretaceous in age based on geologic relations and radiometric dating in adjacent quadrangles of the Ruby Mountains–East Humboldt Range core complex (Sicard and Snoke, 2020).

Domain 2 consists of a sedimentary sequence that range in age from lower Permian to Upper Triassic. This domain is also exposed farther to the north, where the Pennsylvanian Ely Limestone is part of the sequence. This sequence is characterized by low CAIs of 2–2½–3 indicating temperatures of 60–200°C. The structural base of this sedimentary sequence is the southeastern East Humboldt detachment fault, which records brittle deformation characteristic of deformation <300°C. Middle Eocene volcanic and volcanoclastic rocks exposed at the southern end of the East Humboldt Range unconformably overlie upper Permian Park City Group and Lower Triassic Thaynes Formation of domain 2. This relationship indicates that the age of the southeastern East Humboldt detachment fault is younger than middle Eocene (~39 Ma), because there is no evidence that the volcanic and volcanoclastic rocks are deposited on the footwall of the southeastern East Humboldt detachment fault. The sedimentary rocks of domain 2 are

folded and tilted suggesting deformation prior to the deposition of the middle Eocene volcanic and volcanoclastic rocks and subsequent emplacement of the southeastern East Humboldt detachment fault. Domain 2 is also intruded by stocks, sills, and dikes of porphyritic biotite granodiorite inferred to be middle Eocene in age.

The youngest deformation of the rocks exposed in the Arizona Spring quadrangle is normal faults that cut rocks of domains 1 and 2. Although these faults are undated, based on regional relationships, they are <10 Ma and are part of the normal-fault system that bounds the eastern flank of the East Humboldt Range.

INTRODUCTION AND PREVIOUS WORK

The Arizona Spring quadrangle is located ~45 km (~28 mi) south-southwest of the town of Wells, Nevada. It can be accessed by U.S. Highway 93 and Nevada State Route 229 and a complex of dirt roads that cover most of the quadrangle. The quadrangle includes the southeastern end of the East Humboldt Range metamorphic core complex. This core complex has been mapped at the scale 1:24,000 in the following 7.5-minute quadrangles to the north and northwest: Gordon Creek (Sicard and Snoke, 2020), Humboldt Peak (McGrew, 2018), Welcome (McGrew and Snoke, 2015), Secret Valley (Snoke et al., 2021), Tent Mountain (Zuza et al., 2021), Soldier Peak (Snoke et al., 2022), Heelfly Creek (Dee et al., 2015), and Herder Creek (Dee and Ressel, 2016) (fig. 1). The East Humboldt Range core complex is part of the Ruby Mountains–East Humboldt metamorphic core complex, which extends for nearly 90 km (~56 mi) from Harrison Pass in the southern Ruby Mountains to the northern East Humboldt Range near Wells, Nevada. It is a classic core complex that includes (1) a migmatitic infrastructure, (2) hundreds of meters-thick mylonitic shear zone, and (3) a carapace of unmetamorphosed Paleozoic–Triassic sedimentary rocks and middle Eocene volcanic and volcanoclastic rocks. In the Arizona Spring quadrangle, a low-angle detachment fault separates a footwall of metamorphic rocks from the carapace of unmetamorphosed rocks. The structurally deepest rocks in the quadrangle are a sequence of metamorphosed sedimentary rocks, albeit non-migmatitic, but correlate to the high-grade metasedimentary rocks of the East Humboldt Range core complex extensively exposed immediately to the north (e.g., Gordon Creek quadrangle, Sicard and Snoke, 2020). These metasedimentary rocks are correlated to a metasedimentary sequence mapped in the Wood Hills (Thorman, 1970 and Camilleri, 2010), although those metasedimentary rocks reach a higher grade (locally

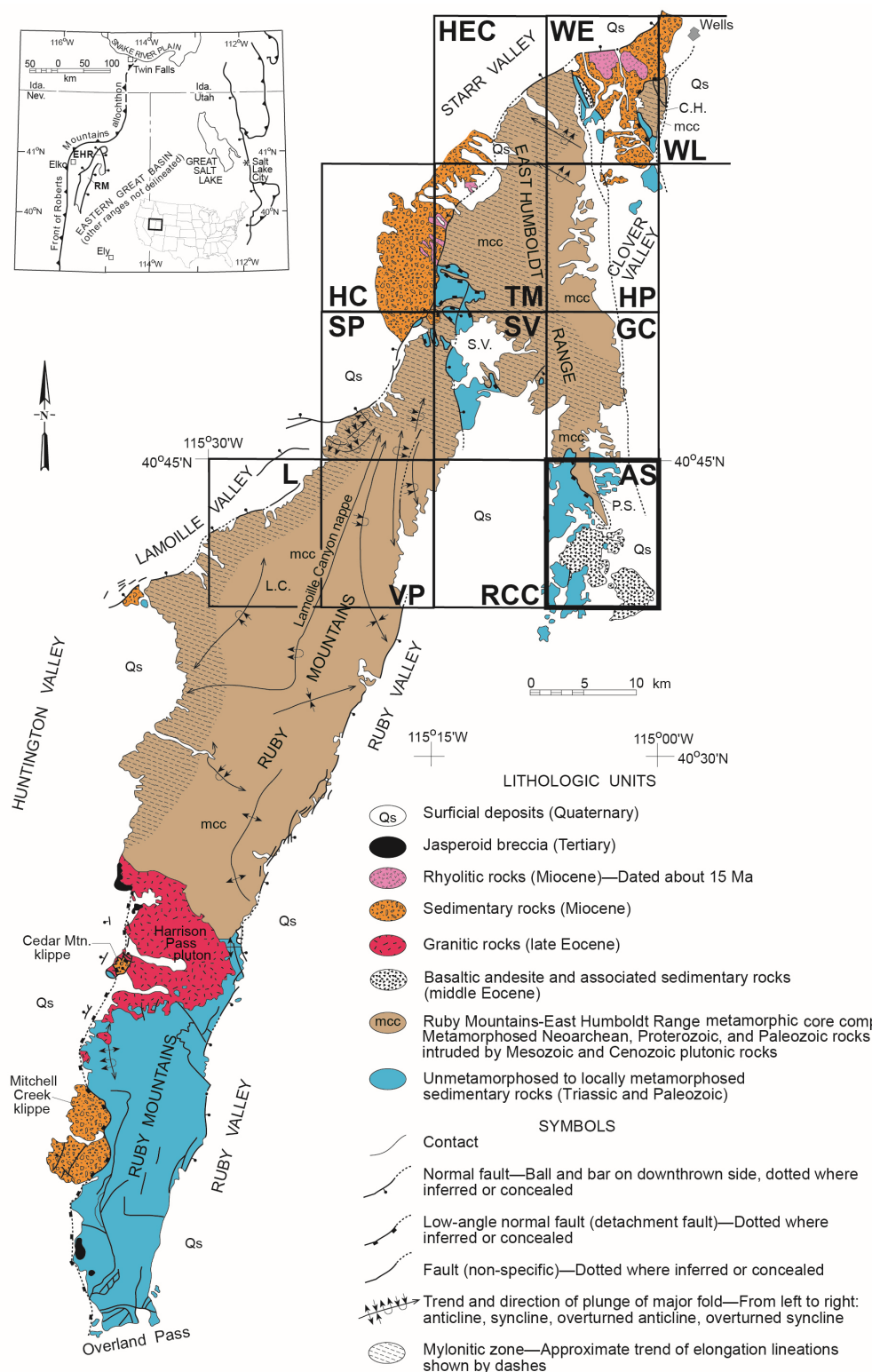


Figure 1 Generalized geologic map of the Ruby Mountains and East Humboldt Range, Nevada. Inset shows map area in relation to other major tectonic elements of the western U.S. Cordillera, including part of the Sevier fold-and-thrust belt and leading edge of the Roberts Mountains allochthon. The names of the 7.5-minute quadrangles are abbreviated as follows: **WE** – Welcome (McGrew and Snoke, 2015), **WL** – Wells, **HEC** – Herder Creek (Dee and Ressel, 2016), **HP** – Humboldt Peak (McGrew, 2018), **TM** – Tent Mountain (Zuza et al., 2021), **HC** – Heelfly Creek (Dee et al., 2015), **GC** – Gordon Creek (Sicard and Snoke, 2020), **AS** – Arizona Spring (this publication), **SV** – Secret Valley (Snoke et al., 2021), **SP** – Soldier Peak (Snoke et al., 2022), **L** – Lamaille (Howard, 2000), **VP** – Verdi Peak (Howard and MacCready, 2004), **RCC** – Ruby City Creek. Other abbreviations are: **C.H.**—Clover Hill; **S.V.**—Secret Valley; **L.C.**—Lamaille Canyon; **P.S.**—Polar Star Mine. Modified from Snoke et al. (1997) and Colgan et al. (2010).

staurolite-kyanite-bearing) than those in the southeastern East Humboldt Range. However, in the southern part of the Gordon Creek quadrangle, kyanite-bearing pelitic schist occurs in the Cambrian–Ordovician marble of Verdi Peak (Sicard and Snoke, 2020).

The earliest detailed mapping in the Arizona Spring quadrangle was included in a Ph.D. dissertation by Snelson (1957). He recognized an undivided Ordovician (?) to Devonian sequence, which he mapped from the Polar Star Mine area to the south-southeast to near Nevada State Route 229, where it crosses the southeastern end of the East Humboldt Range. He described these rocks as recrystallized and contorted and interpreted them to be a thrust slice sandwiched between his subjacent Snow Water unit and overlying Upper Paleozoic to Triassic hanging wall of his Secret Creek thrust. Hope (1970) did reconnaissance mapping in the Gordon Creek and Arizona Spring 7.5-minute quadrangles. He also recognized an Ordovician to Upper Devonian metasedimentary sequence in the southeastern East Humboldt Range. The geologic mapping of Hope is included on plate 1 of the report by Coats (1987). Thorman and Brooks (1994) included a preliminary map of

the southern half of the Arizona Spring quadrangle in a field-trip guide to the area. A portion of the Arizona Spring quadrangle was the subject of a M.S. thesis completed at the University of South Carolina (Taylor, 1984). This thesis included a geologic map of the northwestern part of the Arizona Spring quadrangle at a 1:24,000 scale. The southern part of the quadrangle (south of Nevada Highway 229) has been mapped only in brief reconnaissance.

STRATIGRAPHY

The pre-Cenozoic stratigraphic units in the Arizona Spring quadrangle range from the Cambrian–Ordovician marble of Verdi Peak to the Upper Triassic Shinarump Member of the Chinle Formation. This stratigraphy sequence has been divided into two domains based on age and metamorphic grade. These domains are separated by the southeastern East Humboldt Range detachment fault. The unmetamorphosed sequence (domain 2) includes Pennsylvanian (Gordon Creek quadrangle) to Upper Triassic and is the most complete stratigraphic section

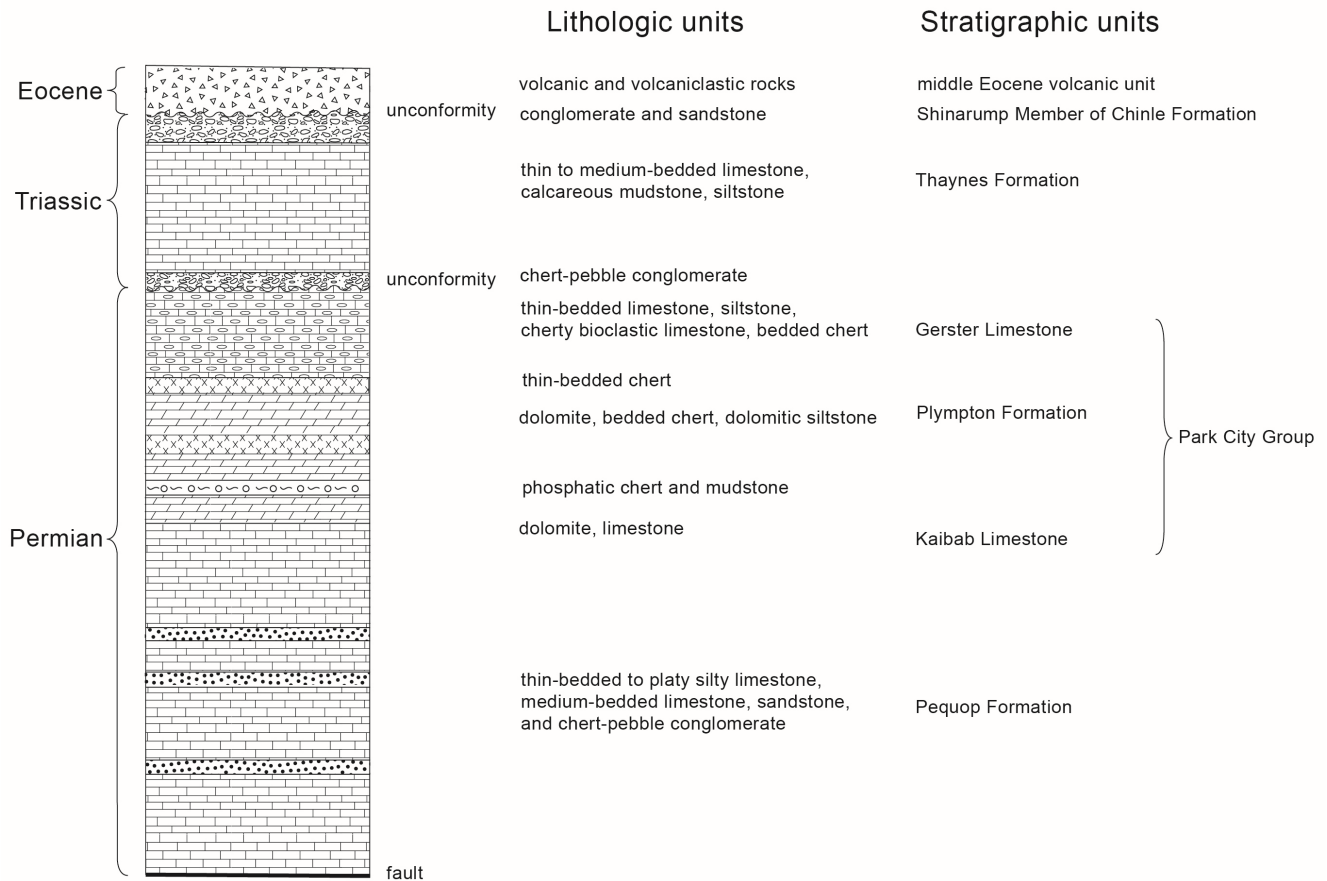


Figure 2 Schematic stratigraphic column of the Paleozoic to early Mesozoic sedimentary rocks of domain 2.

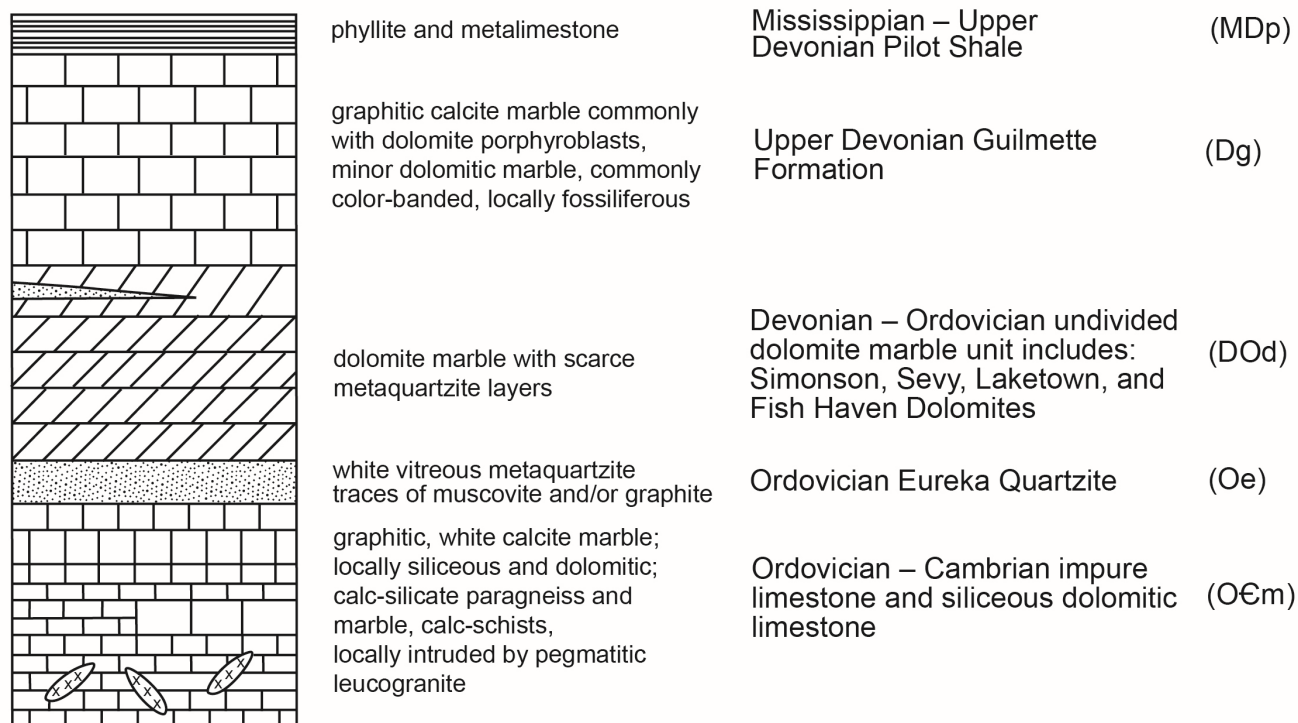


Figure 3 Schematic stratigraphic column of the metasedimentary rocks of domain 1 (after Howard, 1980; Snoke, 1980, and Snoke et al., 1997).

in the upper tier of the East Humboldt Range core complex. The unmetamorphosed units exposed in the Arizona Spring quadrangle are as follows: lower Permian Pequop Formation of Steele (1960), Permian Kaibab Limestone, Permian Plympton Formation with a phosphatic shale member (perhaps equivalent to the Meade Peak phosphatic shale tongue of the Phosphoria Formation), upper Permian Gerster Limestone, Lower Triassic Thaynes Formation and Upper Triassic Shinarump member of the Chinle Formation (fig. 2). The Permian Kaibab, Plympton, and Gerster Formations are part of the Park City Group of western Utah and eastern Nevada (Hose and Repenning, 1959). The metasedimentary rock units of domain 1 are penetratively deformed and metamorphosed, but their distinctive rock types represent mappable stratigraphic units characteristic of the eastern Great Basin (fig. 3). This metamorphic sequence correlates with the metasedimentary rocks mapped in the Wood Hills by Thorman (1970) and Camilleri (2010) and include the Cambrian–Ordovician marble of Verdi Peak, the Ordovician Eureka Quartzite, dolomitic marbles and quartzites of the upper Ordovician Fish Haven and Laketown Dolomites (Richardson, 1913; Hose and Blake, 1976; Thorman, 1970), the Lower to Middle Devonian Sevy and Simonson Dolomites and quartzite (Hose and Blake, 1976), graphitic marbles of the Upper

Devonian Guilmette Formation, and the Mississippian Pilot Shale.

Conodonts from the upper part of domain 2 are characterized by low CAIs from 2–3, indicating temperatures from ~60°C to 200°C. The textures of the sedimentary rocks indicate that they have not experienced metamorphic recrystallization. Conodonts from the metamorphosed Guilmette Formation (domain 1) yielded a CAI of 5, indicating that this marble reached a temperature of ~300°C. In less strained parts of the metamorphosed Guilmette Formation, rounded heads of stromatoporoids (fig. 4A) and spaghetti-like masses of the Coelenterata *Amphipora* (fig. 4B) are distinctive fauna in this formation.

Middle Eocene volcanic and volcanoclastic rocks unconformably overlie the sedimentary sequence of domain 2. These volcanogenic rocks are part of the middle Eocene northeast Nevada volcanic field (Brooks et al., 1995a, b). These rocks do not directly overlie the metamorphosed rocks of domain 1. Associated with these volcanic and volcanoclastic rocks are plugs, sills, dikes, and small stocks of intermediate to granitic intrusive rocks. Scattered hornblende andesitic and microdioritic dikes intrude the sedimentary rocks of domain 2.

Miocene basin deposits (Ts) consisting of sandstone, conglomerate, and tuffaceous sediments occur in the east-

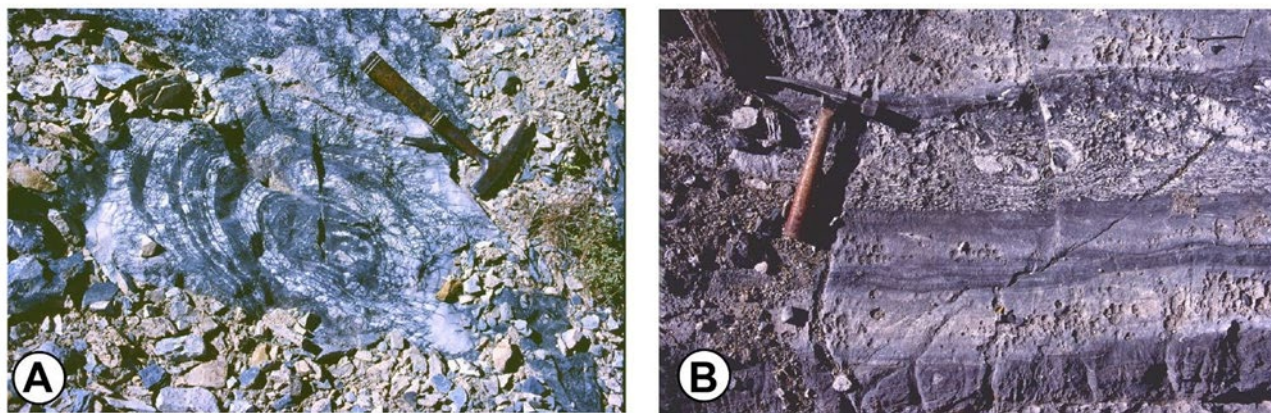


Figure 4 Fossils from the metamorphosed Upper Devonian Guilmette Formation. **A**, Large rounded head of a stromatoporoid. **B**, Spaghetti-like masses of the Coelenterata *Amphipora* with stromatoporoids.

central part of the map area and extend eastward into Clover Valley. These deposits may be correlative with the ~16–10 Ma Humboldt Formation (Colgan et al., 2010).

Quaternary alluvial-fan deposits (Qfy, Qfo, and QTf) cover much of Clover Valley in the eastern part of the quadrangle as well as the piedmont slopes adjacent to the highlands of the southeastern East Humboldt Range. Late Pleistocene lacustrine deposits (Qla and Qlg) in the northeastern corner of the map area were deposited within and adjacent to Lake Clover, which had highstands at approximately 19.5 and 17.0 ka (Munroe and Laabs, 2013).

STRUCTURAL GEOLOGY

The main structural feature in the Arizona Spring quadrangle is the southeastern East Humboldt detachment fault that emplaced younger rocks on older rocks. This low-angle fault is part of the Ruby Mountains–East Humboldt detachment-fault system, which is a major structural feature in the upper tier of the Ruby Mountains–East Humboldt Range core complex. The hanging wall sequence of this fault system (domain 2) varies from lower Permian sedimentary rocks through middle Eocene volcanic and volcanoclastic rocks. To the north in the Gordon Creek quadrangle, the Pennsylvanian Ely Limestone and a small fault-bounded slice of the lower Permian limestone-conglomerate unit are part of the hanging wall sequence (Sicard and Snoke, 2020). The footwall sequence (domain 1) is composed of metasedimentary rocks that range from the Cambrian–Ordovician marble of Verdi Peak to the Devonian–Mississippian metamorphosed Pilot Shale. Taylor (1984) divided the map area into two metamorphic and structural domains separated by southeastern East Humboldt detachment fault.

The detachment fault and associated faults are prominently exposed along the length of the study area particularly along the east-facing flank of main ridge of the southeastern East Humboldt Range. Domain 1 consists of metasedimentary rocks that vary from the Cambrian–Ordovician marble of Verdi Peak to metamorphosed Devonian–Mississippian Pilot Shale (fig. 2). These metasedimentary rocks are polyphase-deformed and range from greenschist to upper amphibolite facies in metamorphic grade. The dominant metamorphic structure is compositional layering and/or penetrative foliation (S1) (fig. 5). Original bedding has been transposed by ductile flow. Rare isoclinal folds (F1) are part of this early deformation. The age of F1 folds in domain 1 is interpreted as synchronous with metamorphism, which is Late Cretaceous based on radiometric dating and crosscutting relations in adjacent quadrangles (Sicard and Snoke, 2020; Snoke et al., 2021; Zuza et al., 2021). The compositional layering and/or foliation (S1) are folded by a second deformational phase forming referred to as F2. Fold hinges of mesoscopic F2 folds are not commonly observed and are inferred by the change in S1 attitudes from outcrop-to-outcrop. On an equal-area, lower-hemisphere projection, poles to S1 form a girdle (fig. 5). The pole normal to the best-fit, great circle defines a fold axis trending approximately 13°/235° (fig. 5B). The hinge zone of a map-scale F2 antiform is present south of Outhouse Draw. Its axial trace plunges to the south and can be mapped northward into the Gordon Creek quadrangle.

Domain 2 includes all the rocks in the hanging wall of the southeastern East Humboldt detachment fault. In the map area, these rocks range from unmetamorphosed Lower

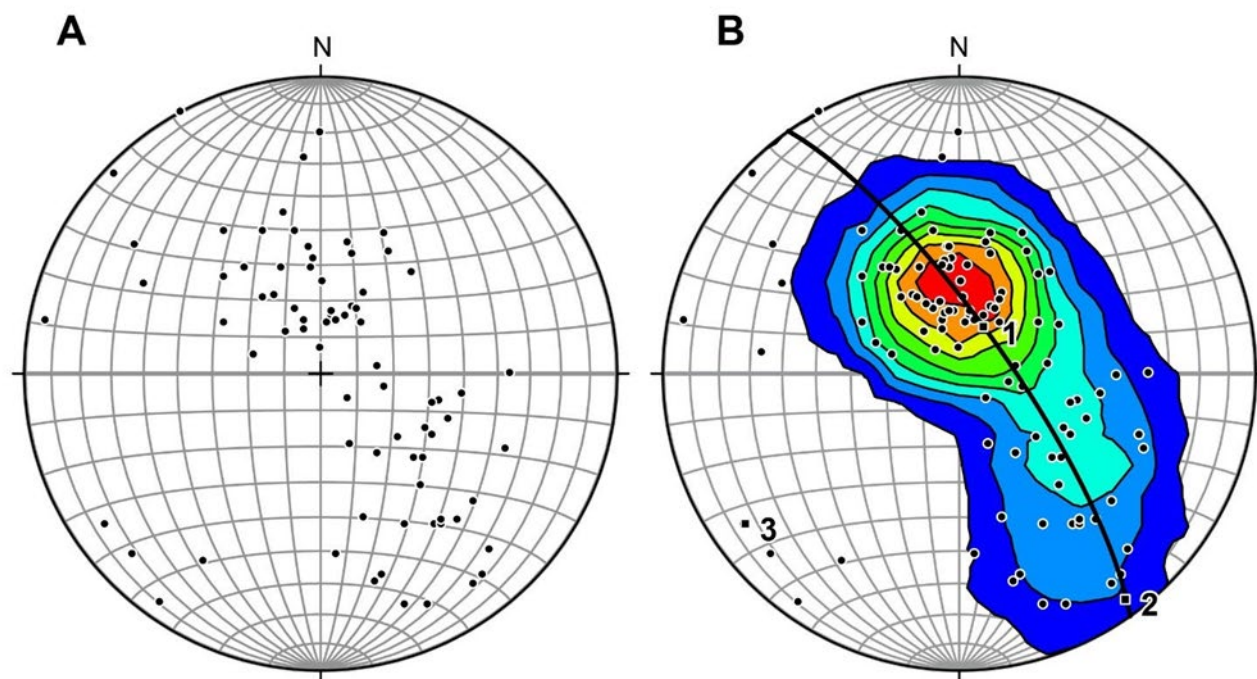


Figure 5 Equal-area, lower-hemisphere projections of structural data from domain 1. **A**, Poles to foliation and compositional layering (filled black circles, $n = 106$). **B**, Poles to planar structures in domain 1 contoured by the Kamb technique. Kamb contours are at intervals of 2σ . The pole to the best-fit great circle indicates an average fold axis of $13^\circ/235^\circ$.

Permian to Lower Triassic sedimentary rocks as well as unconformably overlying middle Eocene volcanic and volcanoclastic rocks. This rock sequence indicates that the southeastern East Humboldt detachment fault must be younger than middle Eocene. The pre-Eocene rocks of domain 2 have been folded, which is interpreted to indicate shortening prior to the development of the southeastern East Humboldt detachment fault and younger tilting and faulting related to crustal extension. The nature of the contact between the Eocene volcanic rocks and the underlying domain 2 rocks is not clear in the study area. The relatively low-lying topography of these volcanic rocks, coupled with their lower resistance to erosion, add to uncertainty in definitive conclusions regarding contacts and attitudes. In the central part of the study area, the Eocene volcanic rocks are generally found proximal to Triassic strata, but, depending on the amount of Cenozoic folding and erosion prior to deposition of the volcanic rocks, an angular unconformity could be present with Eocene volcanic rocks variably deposited on Permian as well as Triassic strata. Alternately, where the volcanic rocks are found proximal to older Permian strata, a normal fault contact may separate them.

Poles to bedding attitudes in domain 2A (west of the Jerry Crab Spring normal fault) plotted on an equal-area,

lower-hemisphere projection (fig. 6A, B) yield a broad scattering of data. The pole normal to the best-fit, great circle defines a fold axis trending approximately $5^\circ/211^\circ$ (fig. 6B). Poles to bedding attitudes in domain 2B (east of the Jerry Crab Spring normal fault) plotted on an equal-area, lower-hemisphere projection (fig. 6C) yield an asymmetric bull's-eye pattern. The pole normal to the best-fit, great circle defines with a fold axis trending approximately $22^\circ/224^\circ$ (fig. 6D).

Reconnaissance mapping south of Nevada Highway 229 (in part by C. Henry, personal communication, 2024) added additional bedding attitudes for domain 2. Poles to bedding attitudes in domain 2 south of Nevada Highway 229 plotted on an equal-area, lower-hemisphere projection (fig. 7A, B) yield a scatter of poles chiefly plunging westward. The pole normal to the best-fit, great circle defines a fold axis trending approximately $14^\circ/172^\circ$ (fig. 7B). Combining all poles to bedding from domain 2, north and south of Nevada Highway 229, (excluding the data set east of the Jerry Crab Spring fault, see fig. 6C, D) are presented in fig. 7C and 7D. The pole normal to the best-fit, great circle defines a fold axis trending approximately $10^\circ/187^\circ$.

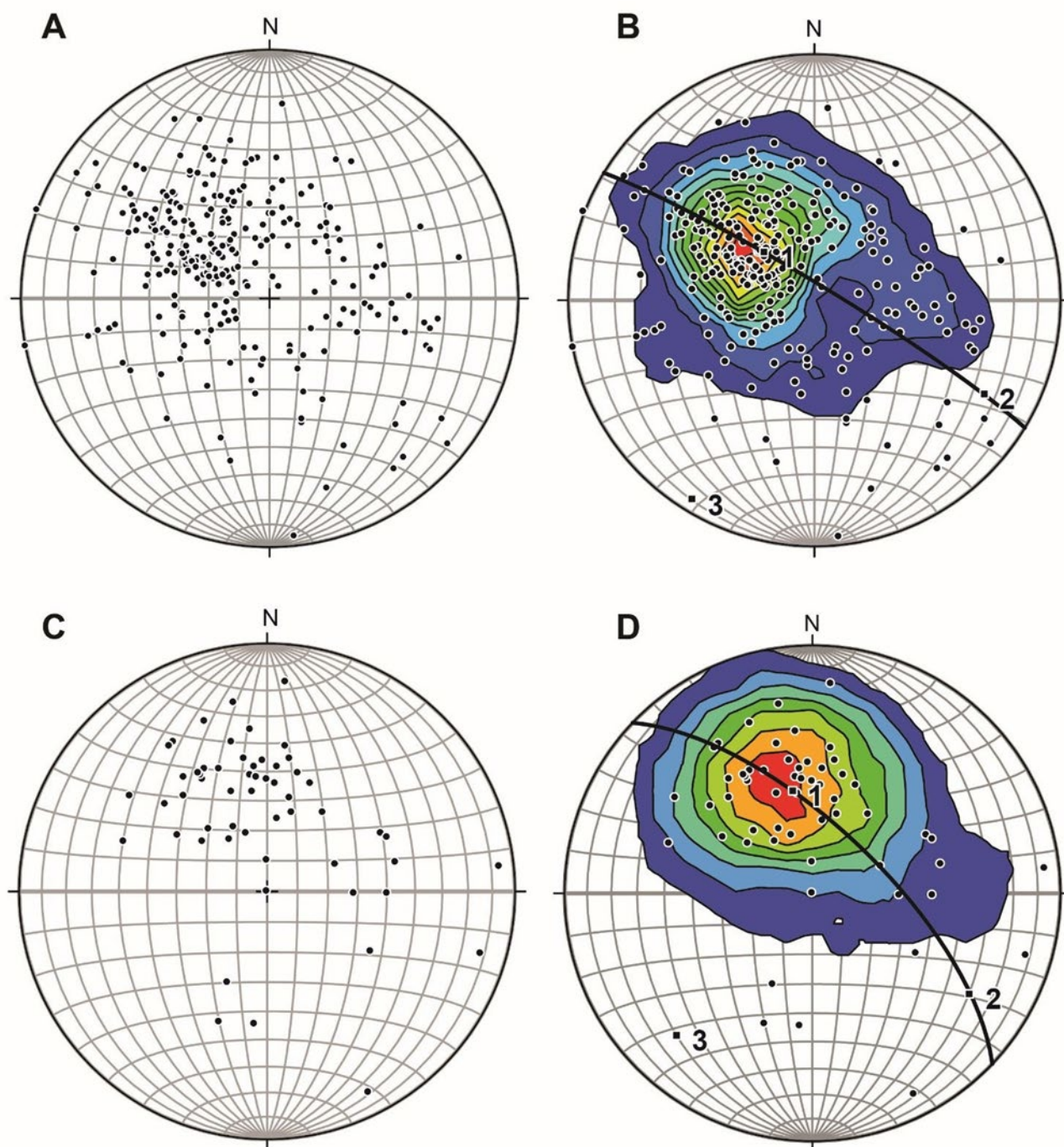


Figure 6 Equal-area, lower-hemisphere projections of structural data from the northern part of domain 2. **A**, Poles to bedding in sedimentary rocks (filled black circles, $n = 267$) west of the Jerry Crab Spring normal fault and north of Highway 229. **B**, Poles to bedding in sedimentary rocks west of the Jerry Crab Spring normal fault contoured by the Kamb technique. Kamb contours are at intervals of 2σ . The pole to the best-fit great circle indicates an average fold axis of $5^\circ/211^\circ$. **C**, Poles to bedding in sedimentary rocks ($n = 56$) east of the Jerry Crab Spring normal fault. **D**, Poles to bedding in sedimentary rocks east of the Jerry Crab Spring normal fault contoured by the Kamb technique. Kamb contours are at intervals of 2σ . The pole to the best-fit great circle indicates an average fold axis of $22^\circ/224^\circ$.

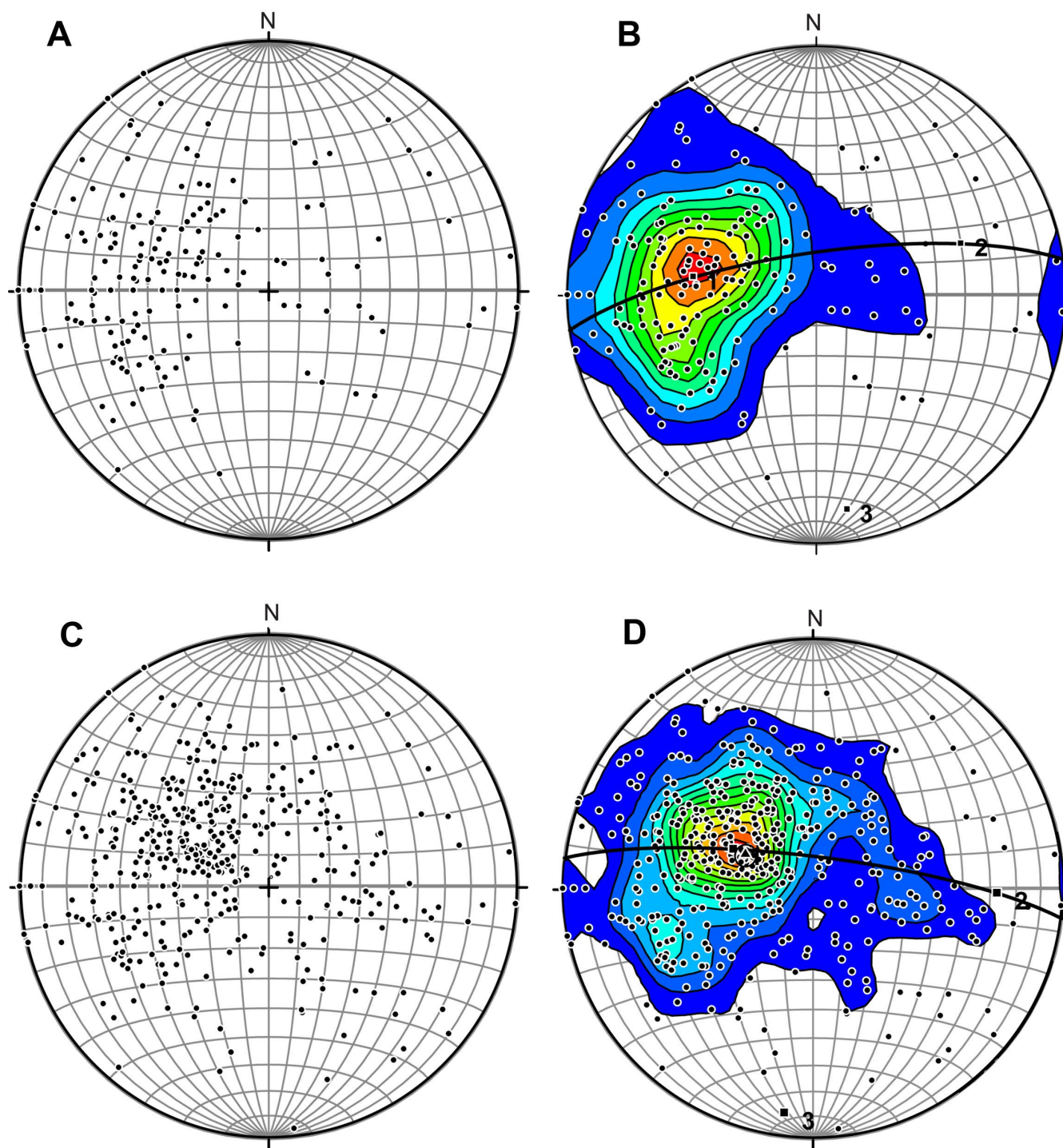


Figure 7 Equal-area, lower-hemisphere projections of structural data from domain 2. **A**, Poles to bedding in sedimentary rocks (filled black circles, $n = 191$) west of the Jerry Crab Spring normal fault and south of Highway 229. **B**, Poles to bedding in sedimentary rocks west of the Jerry Crab Spring normal fault and south of Highway 229 contoured by the Kamb technique. Kamb contours are at intervals of 2σ . The pole to the best-fit great circle indicates an average fold axis of $14^{\circ}/172^{\circ}$. **C**, All poles to bedding in sedimentary rocks ($n = 454$) west of the Jerry Crab Spring normal fault north and south of Highway 229. **D**, Poles to bedding in sedimentary rocks west of the Jerry Crab Spring normal fault north and south of Highway 229 contoured by the Kamb technique. Kamb contours are at intervals of 2σ . The pole to the best-fit great circle indicates an average fold axis of $10^{\circ}/187^{\circ}$.

The most conspicuous structural feature in the map area is the southeastern East Humboldt detachment fault. Although this detachment may be part of Ruby Mountains–East Humboldt detachment-system fault, its age is uncertain and may pre-date the middle Miocene Ruby Mountains–East Humboldt detachment fault exposed in the Secret Valley (Snoke et al., 2021), Soldier Peak (Snoke et al., 2022), and Tent Mountain (Zuza et al., 2021) quadrangles. The detachment fault is the fundamental boundary between domains 1 and 2. The fault is a low-angle, normal fault, which emplaced younger rocks on older rocks. The southeastern East Humboldt detachment fault is prominently exposed along the east-facing flank of the main ridge in the map area. Subordinate low-angle faults, which root into the southeastern East Humboldt detachment fault, bound coherent slices of strata, which are consistently intermediate in age to units above (younger) and units below (older). The presence of folded and eroded Permian and Triassic strata, coupled with low-lying Eocene volcanic rocks and observed on outcrop patterns, strongly suggests (to the senior author) that an angular unconformity exists upon which the volcanic rocks were deposited. The surface of the detachment fault and domain 2 and domain 1, above and below it, have been subsequently uplifted and tilted by younger normal faulting to achieve the current fault surface orientation.

The relationship between the southeastern East Humboldt detachment fault and km-scale mylonitic shear zone exposed to the north in the Gordon Creek quadrangle (Sicard and Snoke, 2020) is uncertain. However, the detachment fault is clearly younger based on the structural style of the two structural features: plastic deformation versus brittle deformation. Nevertheless, these structural features may represent the progressive unroofing of the East Humboldt Range core complex during the middle Tertiary regional extensional deformation in the eastern Great Basin. In the Secret Valley quadrangle Snoke et al. (2021) dated a similar low-angle normal fault as younger than ~17 Ma but older than ~15 Ma. However, the age of the southeastern East Humboldt detachment fault could be older based on the age of low-angle normal faulting in the Spruce Mountain area (Pape et al., 2015). In that area, southeast of the southeastern East Humboldt Range, three distinct low-angle normal faults have been recognized: North Peak, South Peak, and Spruce Spring faults (Hope, 1972; Pape et al., 2015). Mapped relationships of these faults are complex, but the Spruce Spring fault is structurally above and truncates South Peak fault. The South Peak and North Peak faults may be along strike continuation of the same fault. Eocene rhyolite porphyry dikes (~38 Ma, Pape et al. 2016) cut or

intrude the North Peak fault. Thus, this fault was active in the Eocene and indicates an important episode of low-angle faulting prior to the middle Miocene low-angle faulting in the Secret Valley quadrangle.

Middle Eocene volcanic and volcanoclastic rocks are interpreted as part of the hanging wall of the southeastern East Humboldt detachment indicating an age of low-angle, normal faulting younger than ~39–41 Ma. Although intrusive rocks are sparse in the Arizona Spring quadrangle, they are locally cut by high-angle normal faults. Similar intrusive rocks occur in the Spruce Mountain area, which date between 37.3–39.1 Ma, although Middle Jurassic porphyritic dacite has also been dated from the area (Pape et al., 2015). In the Arizona Spring quadrangle, form lines mapped in Eocene rocks are based on topographic and color patterns seen on satellite imagery; their origin and meaning are uncertain.

Domain 2 is complexly overprinted by high-angle normal faults, many of which are too small in displacement to show in map scale. These normal faults do not cut the southeastern East Humboldt detachment fault and consequently developed either prior to or synchronous with detachment faulting. Brecciation and hydrothermal alteration are locally associated with these faults.

The youngest structural feature in the map area are high-angle normal faults related to the Basin and Range. These faults are exposed on the east side of the southeastern East Humboldt Range. The Jerry Crab Spring, Gordon Creek, and Warm Springs high-angle faults can be traced from the Gordon Creek quadrangle (Sicard and Snoke, 2020) into the Arizona Spring quadrangle. The Warm Springs fault displaces Qfo and QTf alluvial-fan deposits and is interpreted to be the bounding fault of the southeastern East Humboldt Range. This fault can be mapped into the middle Eocene volcanic and volcanoclastic rocks south of Nevada Highway 229 where an inlier of Park City Group rocks is on the footwall of the fault. The Jerry Crab Spring fault down drops sedimentary rocks of domain 2, which range from the lower Permian Pequop Formation to the Lower Triassic Thaynes Formation. This same fault cuts a middle Eocene intrusive body in the Outhouse Draw area. The age of the onset of normal faults in the Arizona Spring quadrangle is unconstrained. However, based on regional relations, these faults are probably younger than 10 Ma (Colgan and Henry, 2009; Henry et al., 2011).

CONDITIONS OF METAMORPHISM

The metamorphic sequence, which comprises domain 1, varies in grade from greenschist to amphibolite facies. The

highest-grade rocks are in the Cambrian–Ordovician marble of Verdi Peak. In this unit, calc-silicate paragneiss includes tremolite, scapolite, phlogopitic biotite, and scarce diopside. This mineral assemblage indicates amphibolite facies with metamorphic temperatures $>500^{\circ}\text{C}$ based on the system $\text{CaO-MgO-SiO}_2\text{-H}_2\text{O-CO}_2$ (Spear, 1993). All the metamorphic units in domain 1 have been penetratively deformed and have at least two distinct fold phases. North of the Polar Star Mine, the metamorphic grade of the metasedimentary rocks increases in the marble of Verdi Peak, and bodies of pegmatitic leucocratic become more common as the southern boundary of the Gordon Creek quadrangle is approached. Farther north in the Gordon Creek quadrangle, plutons of pegmatitic leucocratic granite are common (Sicard and Snoke, 2020). The lowest metamorphic grade in domain 1 is a lower-greenschist facies phyllite. This unit is correlate to the Devonian–Mississippian Pilot Shale. The penetrative foliation in the phyllite is commonly crenulated by microfolds (fig. 8).

IGNEOUS ROCKS

Introduction

The igneous rocks in the quadrangle include: (1) a volcanic sequence of lava, flow breccia, ash-flow tuff, and scarce volcanogenic epiclastic rocks (Tvs), (2) hornblende±biotite granodiorite porphyry (Ti), and (3) mafic dikes. The volcanic sequence was originally mapped by Sharp (1939), who assumed that these rocks were Pliocene in age. Snelson (1957) remapped this sequence, which he referred to as the “Warm Springs unit.” He concluded that these volcanic rocks were “Late Tertiary to Pleistocene.” Taylor (1984) reported a K-Ar whole-rock age of 32.5 ± 1.0 Ma was reported (E.H. McKee, personal communication, 1981). More recent studies by Brooks et al. (1995a, b) have conclusively demonstrated an older age of middle–late Eocene for the volcanic sequence. These authors reported three $^{40}\text{Ar}/^{39}\text{Ar}$ dates from andesitic rocks collected at the southern end of the East Humboldt Range. These ages

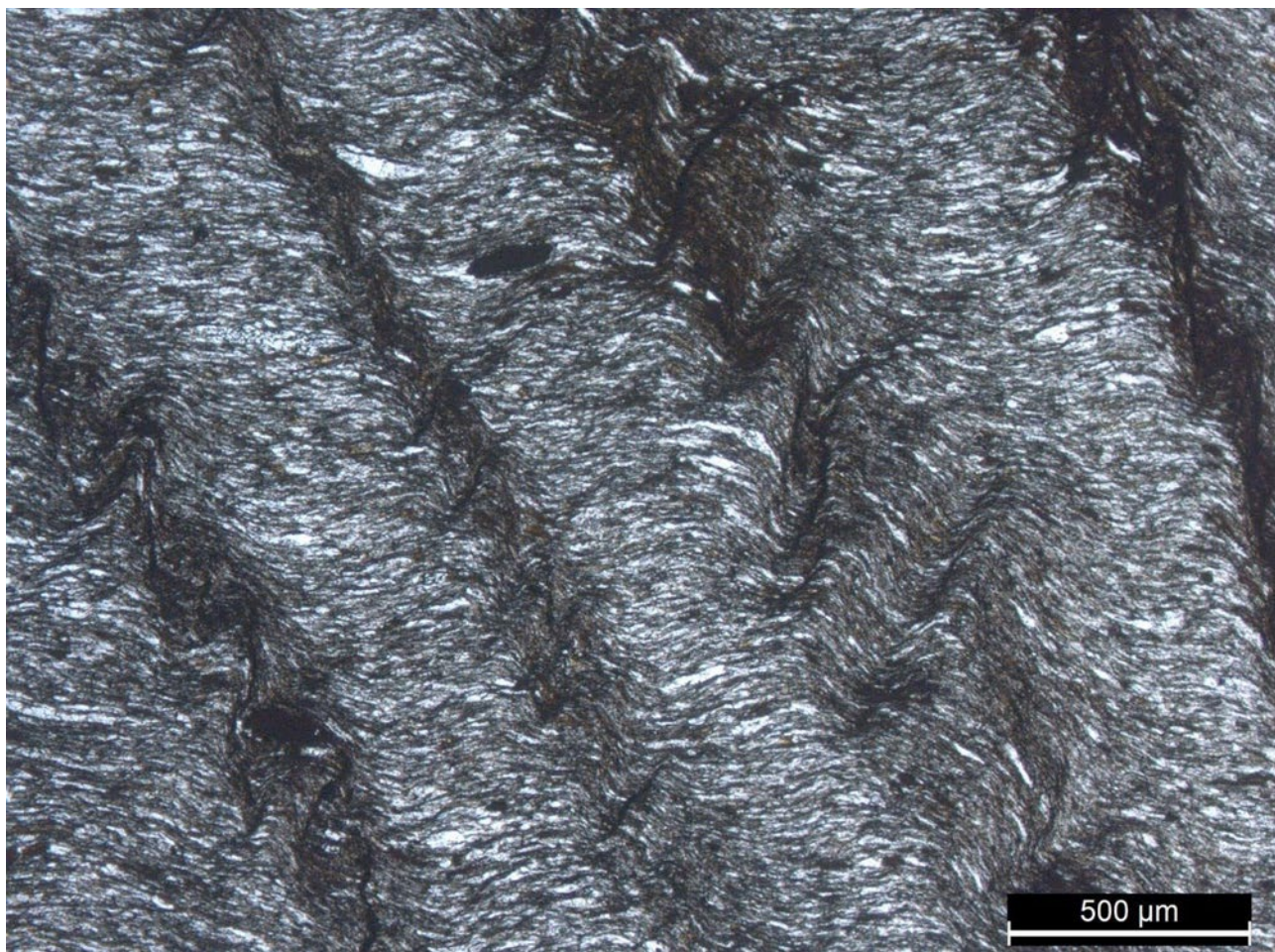


Figure 8 Crenulated phyllite correlated with the Upper Devonian–Mississippian Pilot Shale (Plane Polarized Light (PPL)). Metamorphic grade is lower greenschist facies. The scale in the lower right corner of the photomicrograph is 500 μm .

and the mineral dated are 38.8 ± 0.4 Ma (hornblende, their sample 91T12), 39.5 ± 0.3 Ma (hornblende, their sample 91T17), and 40.98 ± 0.1 Ma (biotite, their sample 91T19). Also, see Brooks et al. (1995b) for whole-rock chemical analyses from the dated samples as well as other samples from this unit (their table 3). Major oxide analyses indicate that the volcanic rocks have a calc-alkaline geochemical signature. Brooks et al. (1995a, b) considered the volcanic sequence exposed at the southeastern end of East Humboldt Range as part of the northeast Nevada volcanic field. The base of the volcanic sequence is an angular unconformity on late Paleozoic and Triassic sedimentary rocks. All these rocks are in the hanging wall of southeastern East Humboldt detachment fault, which is well exposed to the north in the Gordon Creek quadrangle (Sicard and Snoke, 2020). The

angular unconformity indicates an important period of erosion before the middle Eocene and the low-angle normal faulting post-dates the middle Eocene.

Volcanic Sequence (Tvs)

The most common rock types in the volcanic sequence are two-pyroxene basaltic andesite and hornblende±augite andesite lavas (fig. 9A, B). In addition, dacite lava, flow breccia, ash-flow tuff, and scarce volcanogenic epiclastic rocks are also form part of the sequence. The basaltic andesite consists of hypersthene, augite, and calcic plagioclase microphenocrysts (< 1 mm) in a mesostasis of glass, plagioclase microlites, and opaque oxides (fig. 9A). These characteristics indicate a high-temperature, dry magma with no hydrous igneous phases. The hornblende

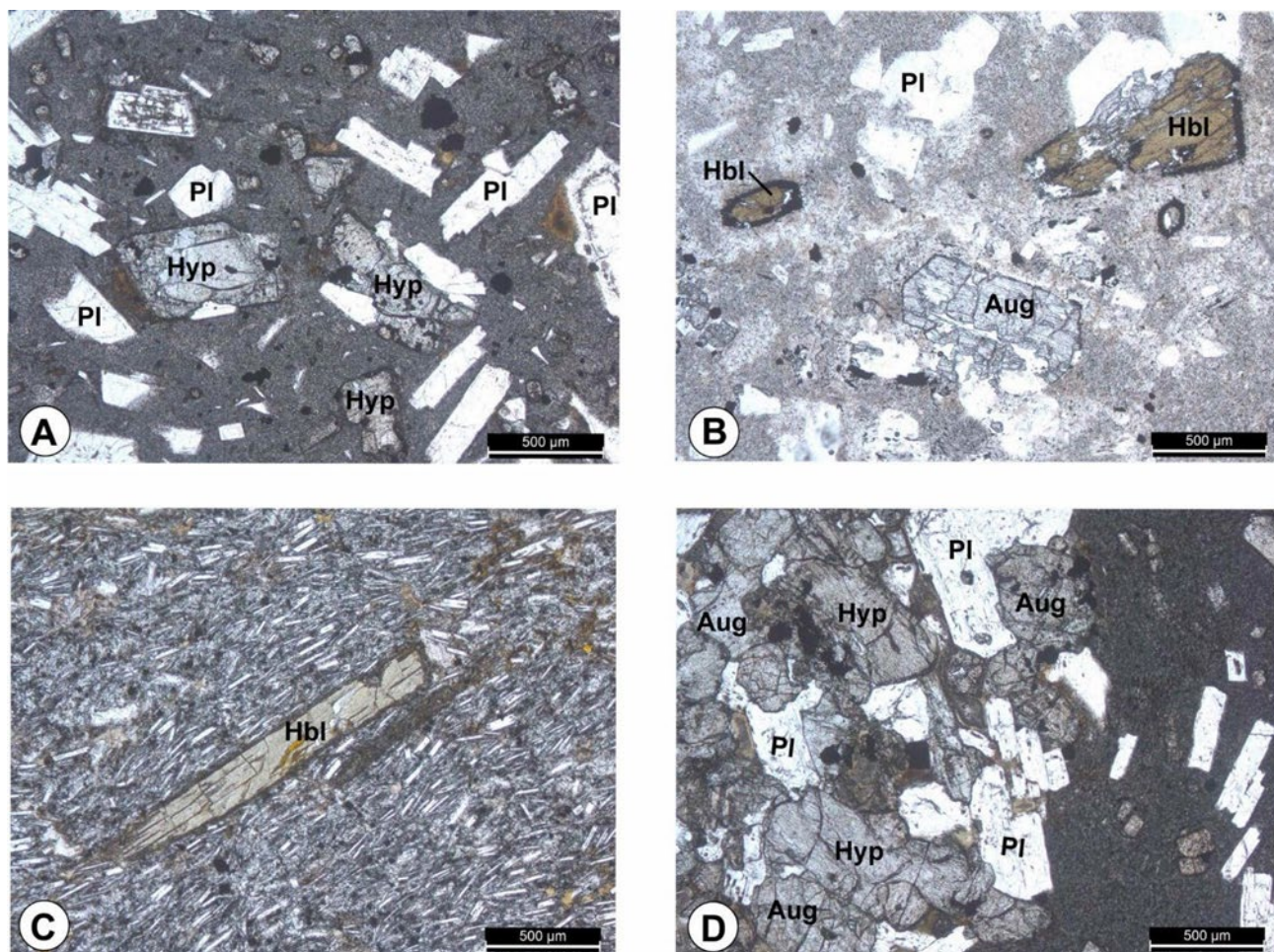


Figure 9 Photomicrographs of samples from the middle Eocene volcanic sequence. **A**, Two-pyroxene andesite (PPL). Both hypersthene and augite (hypersthene > augite) occur in this rock. It is characterized by small phenocrysts of hypersthene, augite, and plagioclase in a fine-grained groundmass consisting chiefly of plagioclase microlites and glass(?). **B**, Augite-hornblende andesite (PPL). Prismatic augite and armoring of hornblende phenocrysts by opaque oxides. **C**, Highly elongated prism of hornblende in trachytic texture consisting chiefly of plagioclase laths (PPL). The trachytic texture defines a flow structure around the hornblende prism. Although not shown in this photomicrograph, multi-crystal clots (glomeroporphyritic texture) of hornblende and augite occur in this rock with the trachytic texture flowing around the clots. **D**, Two-pyroxene andesite with well-developed glomeroporphyritic texture consisting of plagioclase, hypersthene, and augite clots in a fine-grained groundmass shown on the right side of the photomicrograph (PPL). The scale in the lower right corner of each photomicrograph is 500 μ m.

andesite is characterized by olive-brown, prismatic hornblende microphenocrysts, some reaching 2 mm in length (fig. 9C). This rock type has a mesostasis of glass, plagioclase microlite, and opaque oxides. In the hornblende andesite, augite and biotite are subordinate igneous phases. Some of the lavas exhibit a trachytic texture defined by plagioclase laths and prismatic hornblende grains, although some of the hornblende grains are oblique to high angle to the flow fabric (fig. 9C). Sometimes microphenocrysts of hornblende, hypersthene, augite, and/or plagioclase form clumps of grains developing a glomerporphyritic texture (fig. 9D), indicating synneusis during magma flow. Subsequent to the geologic mapping of the Arizona Spring quadrangle (1982–1983), Brooks et al. (1995a) described two volcanic centers. One volcanic center consists of apophyses of pyroxene diorite that intruded and contact metamorphosed Permian and Triassic strata. Two titanite

fractions from the diorite yielded U-Th-Pb ages of 39 ± 0.4 Ma and 37.8 ± 0.3 Ma (R. E. Zartman, personal communication, 1994, reported in Brooks et al., 1995a). Another center consists of several vents based on the presence of near-source block and breccia flows and agglomerate.

Granodiorite Porphyry (Ti)

Scattered throughout domain 2 are numerous small intrusions of porphyritic igneous rocks. The rocks occur as plugs, dikes, sills, and a small stock in the Arizona Spring area. Where possible these occurrences were delineated on the geologic map, although some were too small to show based on the scale of the map.

In fresh samples, conspicuous phenocrysts of hornblende, biotite, plagioclase, and quartz are visible, and the groundmass is aphanitic. Primary accessory minerals

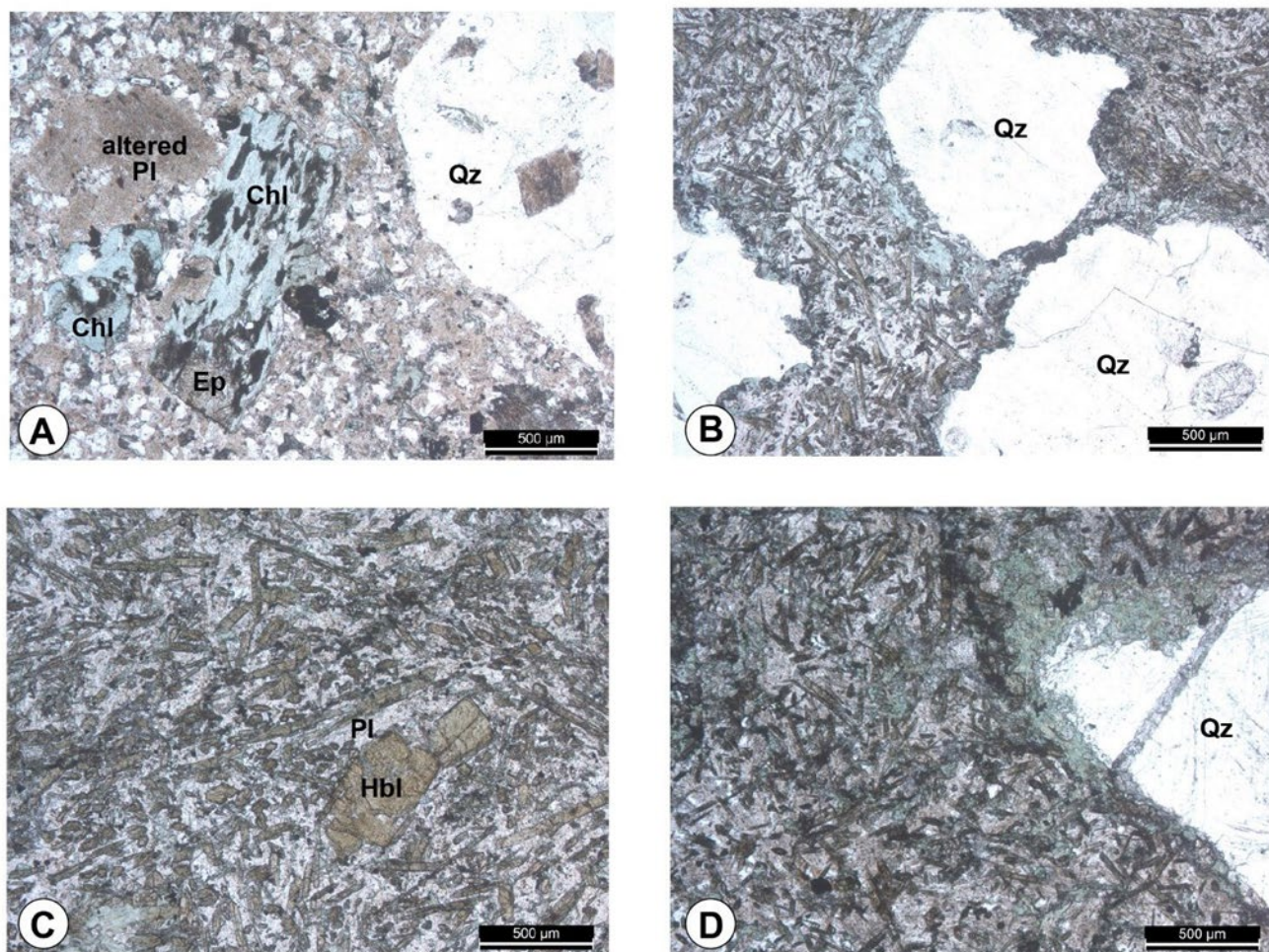


Figure 10 A, Altered hornblende granodiorite porphyry (PPL). A quartz phenocryst is on the right side of the view. Relict hornblende grains are replaced by chlorite, epidote, and leucoxene; plagioclase phenocrysts are altered to sericite and clay minerals. B, Fine-grained mafic dike that contains three xenocrystic quartz grains (PPL). The quartz grains are embayed by the matrix of the host rock. Acicular hornblende grains are characteristic in this rock. C, Fine-grained mafic dike consisting chiefly of acicular hornblende and plagioclase (PPL). D, Another example of a mafic dike (hornblende microdiorite), which contains a large xenocrystic quartz grain cut by a calcite-filled microfracture (PPL). The scale in the lower right corner of each photomicrograph is 500 µm.

include zircon, apatite, and allanite. Alkali feldspar is not a common mineral in these granitic rocks. Post-crystallization hydrous alterations are common in these rocks, where chlorite and epidote replace the igneous phases (fig. 9A). A granophyric texture rarely occurs in the porphyritic igneous rocks, indicating a hypabyssal and rapid crystallization history. The quartz grains are embayed and rounded, probably due to resorption (fig. 9B). Contact relations are generally sharply discordant. Contact metamorphism of the surrounding carbonate wall rocks is locally important, especially near the stock near Arizona Spring, where Park City Group has been metamorphosed to a low-grade marble. The age of this intrusive unit is unknown. A small plug of Jurassic muscovite porphyry was mapped in the Secret Valley quadrangle (Snoke et al., 2021), although this rock type is characterized by distinctive muscovite phenocrysts and a more granitic composition.

The Eocene biotite granodiorite–monzogranite orthogneiss of Horse Creek occurs in the Gordon Creek quadrangle (Sicard and Snoke, 2020) and perhaps is a plutonic equivalent of the granodiorite porphyry.

Mafic Dikes

Mafic dikes are common in the Arizona Spring quadrangle, and they intrude rocks of both domains 1 and 2. These dikes were not mapped in the quadrangle. Similar dikes occur in the Gordon Creek and Secret Valley quadrangles, although are much less common in those areas as in the Arizona Spring quadrangle. These rocks are invariably green in color, which reflects their alteration by chlorite and epidote. They are typically characterized by unoriented, acicular olive brown/green to yellow hornblende (figs. 10C, D). However, a few samples exhibited a flow fabric defined by the hornblende grains. Scattered hornblende phenocrysts occur. Other igneous minerals are plagioclase, quartz, and opaque oxides. The composition of the dikes is intermediate (andesitic or microdioritic), and they definitely could be related to the hornblende andesite lavas in the volcanic sequence. An notable aspect of these dikes is grains of xenocrystic quartz (~1 mm) (fig. 10D). One quartz grain is cut by a calcite-filled microfracture and the margins of the quartz grain are decorated by chlorite alteration (fig. 10D).

DESCRIPTION OF MAP UNITS

Quaternary Deposits

Qc Colluvium (Holocene) Unconsolidated, angular to slightly rounded boulders to pebbles of bedrock in a variably sandy matrix. Commonly 1–5 m thick.

Qay Young alluvium (Holocene) Deposits of silt, sand, and pebble- to cobble-sized gravel in active ephemeral stream channels. Includes subrounded to subangular clasts of primarily carbonate and volcanic rocks with lesser quartzite, derived from the adjacent highlands. Qay deposits are equivalent in age and composition to Qfy deposits and are only mapped separately in confined channels that do not connect to mapped alluvial fans. Thickness is up to ~5 m.

Qls Landslide deposits (Holocene to late Pleistocene) Slope failure deposits with a range of characteristics and compositions. Mapped in two locations on the map sheet. In the northern part of the map sheet is an approximately 300 m x 200 m slumped block in Eureka Quartzite (Oe). The head scarp of the landslide is along the trace of the Jerry Crab Spring fault. The landslide is comprised entirely of angular blocks of quartzite with clast up to 2 m in diameter. Another landslide is mapped in the southern part of the map area along a deeply incised tributary of Spring Creek. Here, an approximately 300 m x 200 m landslide is sourced in old alluvial-fan deposits (Qfo) overlying volcanoclastic rocks (Tvs). This landslide is characterized by jumbled volcanic blocks to 0.5 m diameter surrounded by sand and silt. Both landslides form uneven, hummocky surfaces. Estimated thickness is less than 10 m.

Qfy Young alluvium and alluvial-fan deposits (Holocene to late Pleistocene) Deposits of silt, sand, and pebble- to cobble-sized gravel in active and recently abandoned alluvial fans and active ephemeral stream channels. Includes subrounded to subangular clasts of primarily carbonate and volcanic rocks with lesser quartzite, derived from the adjacent highlands. Qfy varies from coarse-grained deposits within and adjacent to mountainous areas, to fine-grained deposits comprised largely of silt and sand in Clover Valley. Surfaces locally have bar and swale morphology near fan heads and within active channels, otherwise planar to mildly dissected by gully erosion. Inset below adjacent Qfo deposits. Thickness is up to ~5 m.

Qla Lacustrine and alluvial deposits (Holocene to late Pleistocene) Variable deposits of lacustrine silt, clay, and sand; and alluvial silt, sand, and minor gravel. Lacustrine silt was deposited in shallow waters of late Pleistocene Lake

Clover, which had highstands at approximately 19.5 ka and 17.0 ka (Munroe and Laabs, 2013). Alluvial deposits are present in channels and are comprised of reworked lacustrine deposits and distal fan sediments. Exposed thickness of unit is ~2 m.

Qlg Lacustrine gravels (late Pleistocene) Gray to brown deposits of moderately to well sorted pebble- to cobble-sized gravel and sand, in shorelines, beach bars, and spits. Clasts are rounded to subrounded. Soils consist of 20- to 30-cm-thick Bw horizon, underlain by 30–50 cm stage II CaCO₃ horizons (Bk). Snail shells are common. Unit was deposited during highstands and regressive phases of late Pleistocene Lake Clover. Lake Clover reached a maximum elevation of 1729 m at 19.5 ka and 17.0 ka (Munroe and Laabs, 2013). Qlg shoreline deposits are inset into Qfo fan deposits. Exposed thickness of unit is 3+ m.

Qfo Older alluvial-fan deposits (late to early Pleistocene) Coarse-grained alluvial deposits in inactive alluvial fans; typically sandy pebble- to cobble-sized gravel with boulders. Subrounded to subangular clasts of primarily carbonate and volcanic rocks with lesser quartzite, derived from the adjacent highlands. Surface morphology ranges from planar to fully rounded erosional remnants. Locally mantled by an eolian cap. Surfaces are dissected with incised channels up to 7 m deep. Stage II–III CaCO₃ horizons up to 2 m thick that locally form a semicontinuous carbonate-rich layer. Qfo deposits are displaced by the range-bounding normal faults in Clover Valley, including the Warm Springs fault. Maximum thickness is estimated at ~30 m.

QTf Oldest alluvial-fan deposits (early Pleistocene to Pliocene?) Coarse-grained alluvial deposits; typically sandy pebble- to cobble-sized gravel with boulders. Clasts are subrounded to subangular carbonate and volcanic rocks derived from the adjacent highlands. Surfaces are fully rounded erosional remnants perched up to 30 m above active stream channels. Soil horizons are largely stripped; however, litter of pedogenic carbonate suggest remnants of Stage IV CaCO₃ horizons (Bk) of unknown thickness. QTf stratigraphically overlies Ts and with a gradational and conformable contact. Where QTf overlies Tvs the contact may be nonconformable. Exposed thickness of the unit ranges from 5 to ~15 m.

Silicified Rocks

Tj Jasperoid breccia (Pliocene to Miocene) Massive siliceous breccia, commonly re-cemented by quartz, associated with normal-sense fault zones (either high- or low-angle), commonly black to dark or medium gray on a

fresh surface. This unit also includes cream-colored to white siliceous breccia and vuggy siliceous veins. All these siliceous rock types are interpreted as the result of hydrothermal replacement of an original rock.

Tertiary Volcanic, Volcaniclastic, and Sedimentary Rocks

Ts Tertiary basin deposits (Miocene) Sandstone, conglomerate, and tuffaceous sediments deposited in the Clover Valley basin. May be correlative with the ~16–10 Ma Humboldt Formation (Colgan et al., 2010). Thickness of the unit along the western edge of Clover Valley is 80–100 m where it is underlain by Eovs, in the axis of Clover Valley the thickness may exceed 500 m.

Eol Limestone (Eocene) Light gray, medium-grained, irregularly bedded, lacustrine limestone. Forms a thin band interbedded with andesite lavas of unit #vs in the upper part of that sequence. Strike length of examined outcrop is approximately 200 m, but non-examined light-colored areas to north and south could increase to ~1 km.

Eovs Volcanic and volcaniclastic rocks (Eocene) Mostly andesite to dacite lava flows, flow breccias, and associated volcanogenic epiclastic rocks. Includes rocks as mafic as hypersthene-augite pyroxene basaltic andesite (fig. 9A) with common hornblende andesite (fig. 9B). See more detailed descriptions above. Chemical analyses show ranges from 53% to 68% SiO₂ (Brooks et al., 1995b). Propylitic alteration is common in the intermediate volcanic rocks. This volcanic sequence is deposited unconformably on late Paleozoic and late Triassic sedimentary rocks. This unconformity is angular, which indicates an important period of erosion prior to the deposition of the middle Eocene volcanic sequence. ⁴⁰Ar/³⁹Ar dates (table 1): 91T12 dacite lava; 39.30±0.80 Ma, hornblende. 91T17 dacite lava 40.01±0.60 Ma, hornblende. 91T19 dacite clast in gravel in Eovs, 41.51±0.20 Ma, biotite. The older apparent age of sample 91T19 suggests it is reworked from a different, older volcanic sequence upstream in the paleovalley that contains the Eocene units. U-Pb zircon date AZ8-18-22 (1), dacite lava 40.1±0.4 Ma.

Eot Ash-flow tuff (Eocene) Light gray, sparsely porphyritic, moderately welded, rhyolite ignimbrite (ash-flow tuff). Phenocrysts of plagioclase (10%, to 1 mm), quartz (3%, to 1 mm), hornblende (1%, to 0.7 mm) biotite (<1%, to 0.5 mm), and sparse sanidine. Forms low outcrops and lag overlying Eocene sedimentary deposits (Eos) and apparently underlying Eocene volcanic and volcaniclastic rocks (Eovs) near the base of the latter. Possibly more extensive in the

very poorly exposed volcanic sequence of the Arizona Spring quadrangle. Sanidine $^{40}\text{Ar}/^{39}\text{Ar}$ dating of sample H23-W288 reveals two populations (table 1). One yields an age of 39.512 ± 0.121 Ma and K/Ca of 106.7 ± 3.0 (table 1), which is the best estimate of eruption age. A second population yields 40.076 ± 0.122 Ma and K/Ca of 71.2 ± 2.1 , which matches the tuff of Big Cottonwood Canyon (Henry, 2008). We interpret this older population to be xenocrysts from the tuff of Big Cottonwood Canyon and suggests unit **Eot** was a late eruption from the Big Cottonwood Canyon caldera, which is about 125 km northwest of the Arizona Spring quadrangle (Henry, 2008). However, no ignimbrite of this age has been recognized in northeastern Nevada. The ignimbrite eruption age overlaps within analytical uncertainty with the $^{40}\text{Ar}/^{39}\text{Ar}$ ages of the two **Eovs** lavas and is only slightly outside uncertainty with the U-Pb date of sample AZ8-18-22 (1) (table 1).

Eos Conglomerate (gravel) and sandstone (Eocene) Conglomerate (gravel) consisting of a lag of well-rounded to subrounded clasts, mostly of Permian and Triassic limestone and dolomite to 50 cm (rarely to 1 m) diameter and varicolored chert to 20 cm. All in dark, clayey soil. Upper part consists of poorly exposed, thick-bedded, tuffaceous to calcareous, white to tan to light red sandstone and platy siltstone composed of quartz, feldspar, biotite, and rock fragments, and locally containing gastropods. Unit is sporadically exposed below volcanic and volcanoclastic rocks (**Eovs**) and overlying Triassic Thaynes Formation (**Trt**) with angular unconformity. The lowermost part of a sedimentary-volcanic sequence may have filled a paleovalley cut into pre-Cenozoic rocks. Undated except underlies definite Eocene ash-flow tuff (**Eot**) and lavas (**Eovs**).

Sedimentary Rocks

Trs Shinarump Member of Chinle Formation (Late Triassic) Conglomerate (fig. 11) and sandstone.

Trt Thaynes Formation (Early Triassic) Gray to chocolate brown, thick-bedded to laminated limestone, bioclastic limestone, siltstone, sandstone, and dolomite (fig. 12). Conglomerate containing clasts of chert and silicified fossil fragments, similar to constituents in the underlying upper Permian Gerster Limestone, locally occurs near the base of the formation interpreted as a regional disconformity (Collinson et al., 1976). Conodont fragments were recovered by Anita G. Harris (U.S. Geological Survey, written commun., 1984) from limestone samples collected at localities 1, 2, and 3. The determined CAIs are 2 ½, 2–3, and 2, respectively, indicating that these limestones reached 60–

150 °C. At locality 3, the conodont *Furnishius triserratus* (Clark) was recovered. This conodont is restricted to the lower and middle Smithian (late Early Triassic).

The Thaynes Formation occurs in two separate areas. The first area is located in the south-central part of the map area occupying much of the low-lying country situated between the main East Humboldt ridge to the west and a lower ridge to the east. The western exposure of this area of Thaynes Formation unconformably overlies the Gerster Limestone. To the east, the Thaynes Formation is in low-angle fault contact with the metasedimentary rocks of domain 1 or Lower Permian Pequop Formation, which is exposed in a fault-bounded low-angle fault slice subordinate to the southeastern East Humboldt detachment fault. The variation of the attitudes in the Thaynes Formation suggested that it has been complexly folded. The second exposure of Thaynes Formation is in the northeastern part of the map area, where it also occurs in an area of low relief. Its western contact is a high-angle normal fault, which juxtaposes Thaynes Formation against metasedimentary rocks of domain 1. This fault tracks to the north into the Gordon Creek quadrangle, where it is mapped as the Jerry Crab Spring fault (Sicard and Snoke, 2020). The Thaynes Formation is unconformably overlain by middle Eocene volcanic and volcanoclastic rocks. To the south and east, the Thaynes Formation is overlain Quaternary alluvium (**Qfo**).

Ppc Park City Group, undivided (late Permian) Light-gray dolomite with white nodular and lenticular chert, light-gray to white limestone with white nodular chert, bedded chert, phosphatic shale, siltstone, and fine-grained sandstone. This undivided unit is interpreted as a composite of the Kaibab Limestone, Plympton Formation, and Gerster Limestone, which comprise the Park City Group in northeastern Nevada (Wardlaw and Collinson, 1978). For the full Park City group (Kaibab, phosphatic member, Plympton, and Gerster) they respectively are: Pk - 225m; Phosphatic member - 25m; Ppcp (Plympton) - 200m; Gerster - 80 m. Total estimate for the Park City group is 530 m.

Pg Gerster Limestone (late Permian) Light brownish gray, thin- to thick-bedded limestone with nodular chert and silicified brachiopods, crinoidal parts, bryozoan, inter-beds of siltstone and fine-grained sandstone, and discontinuous beds of light-gray dolomite locally occur near the base and top of the formation. Conodont fragments *Merrilina* cf. *M. Divergens* (Bender and Steppel), *Neogondolella Wilcoxi* (Clark and Behnken), *Neogondolella* sp. indet., and



Figure 11 Photograph of conglomerate in the Upper Triassic Shinarump Member of the Chinle Formation (T_s).



Figure 12 Photograph of tilted, bedded limestone of the Lower Triassic Thaynes Formation. Hammer is in the left center of the photograph.



Figure 13 A, Looking north at the Permian Park City Group section. Upper Permian Gerster Limestone forms the top of the main ridge of the quadrangle. The Polar Star road (west side of quadrangle) is visible in the lower part of the photo. **B**, Looking north at the cliff-forming, Permian Plympton Formation on the main ridge east of Arizona Spring hill.

Xaniognathus sp. indet. were recovered by Bruce R. Wardlaw and R. Thomas Lierman (U.S. Geological Survey, written commun., 1986) from a limestone sample collected at locality 4. The determined CAI is 3, indicating that this limestone reached at least 200°C. The determined age is Late Wordian (early late Permian).

The Gerster Limestone is best exposed along the top and east-facing slopes of the main ridge of the southern East Humboldt Range in the western part of the map area (fig. 13A). Another coherent section of Gerster Limestone occurs ~2.3 km (~1.4 mi) north of the Polar Star Mine, where it is juxtaposed to Cambrian–Ordovician marble of Verdi Peak of domain 1 by a N–S-striking, high-angle normal fault (Jerry Crab Spring fault). The lower contact of the Gerster Limestone and Plympton Formation is conformable. As limestone with the Thaynes Formation is an erosional disconformity (Collinson et al., 1976). There is variation in the thickness of the Gerster Limestone throughout the map area. Thorman and Brooks (1994) interpreted the contact between the Park City Group and Thaynes Formation as an attenuation fault (their figure 2). However, we have not identified this type of faulting during our mapping. The thickness variations may be related to erosion and internal folding or faulting of the unit.

The basal part of the Gerster Limestone is characterized by the occurrence of massive, cliff-forming cherty limestone (packstones) (fig. 13B). Locally, a basal light-gray dolomite, similar to dolomites of the Plympton Formation, is present. Above the basal packstones, the Gerster Limestone is dominated by interbedded platy, yellow- and reddish-weathering siltstones and fine-grained sandstones, and silty limestone (wackestones and packstones). Limestones in the upper parts of the formation are siltier and characterized by abundant large bryozoans. Locally, at the top of the Gerster Limestone are discontinuous beds of light-gray to tan-weathering dolomite. This relationship suggests that the discontinuous nature of the dolomite is due either to lateral facies variations or differential erosion prior to the deposition of the Triassic rocks.

Ppl Plympton Formation (Permian) Dolomite with yellow-weathering nodular and lenticular chert (fig. 14), bedded chert, dolomitic siltstone, and fine-grained sandstone. A phosphatic shale unit (**Pph**) is delineated at the base of the formation. This unit is inferred to be equivalent to the Meade Peak phosphatic shale tongue of the Phosphoria Formation (Wardlaw and Collinson, 1978).

The basal units of the Plympton Formation are laterally consistent throughout the map area and consist of, in

ascending order, a phosphatic shale and chert, massive dolomite, and fine-grained dolomitic sandstone. The phosphatic unit forms a distinctive saddle consisting of a zone of black shale, mudstone, and orange, brown, and black chert, which contain pelletal phosphorite as small orbs of bluish-white-weathering collophane. Although actual outcrops of this unit are virtually nonexistent, the float is highly characteristic, and the upper and lower contacts are defined by massive dolomites. Small bodies of hypabyssal intrusions of porphyritic biotite-hornblende granodiorite occur in this unit (see description for ‘Igneous Rocks’).

Directly above the phosphatic shale is a 5- to 10-meter-thick, massive fine-grained dolomite. Above the massive dolomite is a slope-forming, yellowish to buff colored fine-grained dolomitic sandstone. Above the sandstone is a poorly exposed sequence of massive chert, cherty light-gray dolomite, fine-grained sandstone, and sedimentary breccia. The breccia contains dolomite and chert fragments set in a veined calcite matrix. Above the breccia zone are five distinctive units that are characteristic of the Plympton Formation throughout the map area: massive dolomite, fine-grained calcareous sandstone, laminated chert, chert-pebble-bearing dolomite, and a thick sponge spicule-bearing massive chert. The top of the Plympton Formation is defined as the top of the spicule-bearing chert.

Pk Kaibab Limestone (Permian) Light to dark gray, thick-bedded limestone and dolomitic limestone, light gray to bluish gray massive dolomite with various amounts of yellow to brown nodular chert. The Kaibab Limestone is exposed along the west face of the main ridge of the southern East Humboldt Range. Exposures of the Kaibab Limestone are also found on the south-facing slopes of the east-trending ridge located ~2.5 km (~1.6 mi) north-northeast of the Polar Star Mine. At this locality, a low-angle normal fault is mapped between the Kaibab Limestone and Pequop Formation and is also exposed in the Gordon Creek quadrangle (Sicard and Snoke, 2020).

The Kaibab Limestone represents the transition from the limestone-dominated rocks of the Pequop Formation to the dolomites of the Plympton Formation. The lowest beds of the Kaibab Limestone, overlying the chert-pebble conglomerate of the uppermost Pequop Formation, are dark gray to black, veined wackestone or micrite, commonly containing crinoids, bryozoan, and large brachiopods. Progressing up section, limestone becomes scarce and dolomite is the dominant rock type. The dolomite is generally light to medium bluish gray and contains variable amounts of nodular chert, which weathers to shades of



Figure 14 Photograph of overturned dolomite with nodular and lenticular chert layers of the Permian Plympton Formation. Direction of view is to the NNE.



Figure 15 Chert-pebble conglomerate at the top of the Lower Permian Pequop Formation. Chert pebbles, left of the hammer head, are partially covered by yellow lichen. This bed is fining upward.

orange, brown, and yellow. The highest unit in the Kaibab Limestone is a 5- 10-meter-thick massive dolomite. Above this dolomite is a distinctive, saddle-forming phosphatic shale, which forms the basal unit of the overlying Plympton Formation.

Pp Pequop Formation of Steele (1960) (early Permian)

Purplish-gray, platy (slope-forming) silty limestone and massive- to thick-bedded, medium- to dark-gray, fine-grained limestone; locally fusulinid-rich coquina; yellow-weathering, calcareous fine-grained sandstone; chert-pebble conglomerate at the top of the formation (fig. 15). In the map area, there are four main exposures of the Pequop Formation. The first, and most complete section is in the northwestern corner of the quadrangle along the main crest of the southeastern East Humboldt Range and associated west and east flanks. Bedding generally strikes northeast and dips southeast at moderate angles (20–40°), although occasionally steeper (~60°). The upper contact is the conformably overlying Kaibab Limestone. The lower contact is the southeastern East Humboldt detachment fault exposed in the Gordon Creek quadrangle (Sicard and Snoke, 2020).

The second exposure of Pequop Formation is located on an east-trending ridge ~3.0 km (~1.86 mi) north-northeast of the Polar Star Mine. Beds generally strike east–west and dip to the south. However, minor folding locally distorts these attitudes. The lower boundary is the southeastern East Humboldt detachment exposed in the Gordon Creek quadrangle (Sicard and Snoke, 2020). The upper boundary is a low-angle fault that places an abbreviated section of Kaibab Limestone on top of Pequop Formation.

The third exposure of the Pequop Formation is located on a hill just southwest of the Polar Star Mine. This package of Pequop Formation is a tectonic slice sandwiched between the southeastern East Humboldt detachment and a subordinate low-angle fault, which places rocks of the Thaynes Formation on top of the Pequop Formation, indicating significant stratigraphic separation.

The fourth exposure of the Pequop Formation is located in the southwest and south-central part of the map area, but only reconnaissance mapping in this area has been conducted (C. Thorman, 2024, personal communication). Thickness estimated at 225 m, complete section is not exposed.

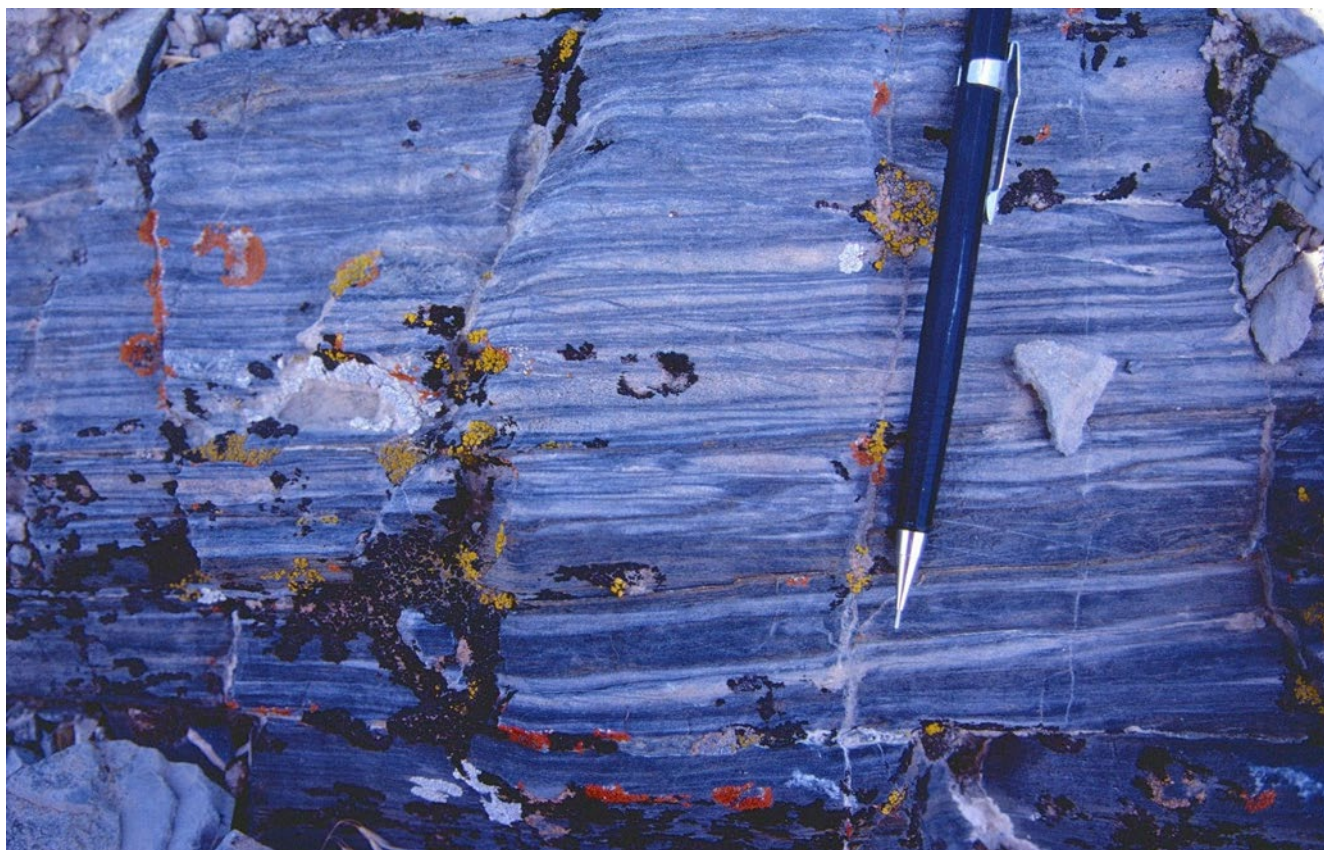


Figure 16 Strongly deformed, metamorphosed Upper Devonian Guilmette Formation. This graphitic calcite ± dolomite marble shows transposition of original bedding.



Figure 17 Coarse-grained vein of scapolite in the Guilmette Formation.

Metamorphosed Sedimentary Rocks

MDp Metamorphosed Pilot Shale (Mississippian to Late Devonian) Black graphitic phyllite with crenulation cleavage, which overprints a penetrative schistosity (fig. 8); interlayered gray metalimestone. The metamorphosed Pilot Shale is very poorly exposed, but is characterized by graphitic phyllitic float, which contrasts sharply from the marble of the Guilmette Formation. The phyllite has a prominent S1 cleavage that commonly is overprinted by a S2 crenulation cleavage.

Dg Metamorphosed Guilmette Formation (Devonian) Fine-grained, strongly deformed, graphitic calcite-dolomite marble (fig. 16) to weakly metamorphosed limestone. Graphite-rich stylolitic seams are common in some samples of the marble. Coarse-grained veins of scapolite locally occur in the marble (fig. 17). The meta-limestone is typically dark gray to black, massive-bedded, and highly veined by calcite. Rounded heads of stromatoporoids (fig. 4A) and spaghetti-like masses of the coelenterata *Amphipora* (fig. 4B) are distinctive fauna in this formation and are even recognizable in metamorphosed and plastically deformed rocks of this

unit. Conodont fragments were recovered by Anita G. Harris (U.S. Geological Survey) from a low-grade fossiliferous, black calcite marble sample collected at locality 5. The determined CAI is 5, indicating that this marble reached ~300°C. Dg thickens north to south, from 50m or less to 225m or more. In fact this thinning to the north is also seen in DOD and Oe as you get into the Gordon Creek quad. Likely same is true of O ϵ m but the base is not exposed so hard to estimate other than the estimate of thinning I provided below in the O ϵ m comment

DOD Dolomitic marble, undivided (Devonian to Ordovician) White to dark gray, fine- to medium-grained, massive dolomitic marble with subordinate metasandstone layers (locally mappable, see below). This undivided unit is correlated with the Middle Devonian Simonson Dolomite, Lower Devonian Sevy Dolomite, Silurian Laketown Dolomite, and upper Ordovician Fish Haven Dolomite. A metasandstone horizon in the upper part of the DOD unit is correlated with sandstone member in the Simonson Dolomite.

Oe Metamorphosed Eureka Quartzite (Ordovician) White vitreous metaquartzite commonly free of impurities

except trace amounts of graphite, muscovite, and/or feldspar; gray (graphite-bearing) metaquartzite may be interlayered with the white metaquartzite. 10–20 m thick.

O₂m Marble of Verdi Peak, undivided (Ordovician to Cambrian) Light gray to yellow tan-weathering micaceous calcite marble and white calcite marble. Common accessory minerals are phlogopite, graphite, muscovite, quartz, and dolomite. Calc-silicate-bearing (chiefly tremolite, diopside, and scapolite), phlogopitic biotite calcite marbles, and calc-silicate paragneiss are locally common. This unit is well-exposed in the Gordon Creek quadrangle (Sicard and Snoke, 2020) where it is complexly intruded by Cretaceous–Tertiary pegmatitic leucogranite. Some exposures of leucogranite occur in this unit in the Arizona Spring quadrangle, although they are not pervasive as to the north in the Gordon Creek quadrangle (Sicard and Snoke, 2020). Thickness of the impure calcite marble in the study area is unknown, but an estimate on the degree of thinning can be obtained if the discontinuous pelitic schist lenses are equivalent to the Kanosh shale. The lenses of schist lie approximately 20–30 meters below the metamorphosed Eureka Quartzite in the map area. Thorman (1970) reported a thickness of 690 feet for the same interval in an unmetamorphosed section of the Pequop Mountains. To the south, in White Pine County, Hose and Blake (1976) report the unmetamorphosed interval to be 200–400 feet thick. These differences suggest thinning of an order of magnitude for the unit in the study area.

Intrusive Rocks

E₂d Diorite and porphyritic andesite intrusions (Eocene) A petrographically heterogeneous suite of mostly intermediate intrusions forms many sills, dikes, and irregular bodies in the southwestern part of the quadrangle. Porphyritic microdiorite with phenocrysts of plagioclase (12 mm, 20%), pyroxene (1 mm, 5–10%), \pm biotite (1 mm, 5%) in a fine groundmass is most common and forms the largest intrusions. Porphyritic andesite with plagioclase and pyroxene phenocrysts in an aphanitic groundmass forms dikes and the margins of the larger intrusions. Common propylitic alteration with chlorite replacing pyroxene and biotite. Inclusions of a coarse granodiorite with abundant biotite to 1.5 cm occur at several places in the largest intrusion and in the small body in the core of the north-striking anticline in Plympton Formation. Age: Brooks et al. (1995b) reported a written communication from Robert E. Zartman of two sphene U-Th-Pb dates of 39.5 ± 0.4 and 37.8 ± 0.3 Ma from the same sample 91T22 diorite intrusion (table 1). The older age, which matches the dates on **E₂vs**, is

probably the best estimate and is consistent with these intrusions being the subvolcanic equivalent of the lavas and volcanoclastic rocks. Brooks et al. (1995a) described a pyroxene diorite that intruded and contact metamorphosed Permian and Triassic strata.

E₂g Granodiorite (Eocene) Hornblende-biotite granodiorite that occur as small intrusive bodies such as plugs, sills, dikes, and small stocks in domain 2. In hand specimen, these rocks are light tan to pinkish-white and are commonly very weathered. These intrusive rocks are porphyritic and locally exhibit a granophyric texture indicative of a shallow emplacement. Phenocrysts include hornblende, biotite, plagioclase, and quartz. The groundmass is aphanitic.

SUMMARY AND CONCLUSIONS

The Arizona Spring quadrangle exposes the upper tier of the East Humboldt Range core complex, which is comprised of a stratigraphic sequence that ranges from Pennsylvanian (exposed in the adjacent Gordon Creek quadrangle immediately to the north) to Upper Triassic rocks (domain 2). These unmetamorphosed rocks occur in the hanging wall of the southeastern East Humboldt detachment fault. The footwall of this low-angle normal fault is a metasedimentary sequence that ranges from Cambrian to Upper Devonian–Mississippian and has been metamorphosed from greenschist to amphibolite facies (domain 1). The highest-grade rocks in this sequence occur in the Cambrian–Ordovician marble of Verdi Peak, where scarce diopside occurs in calc-silicate paragneiss. Small intrusions (< 3 m) of pegmatitic leucogranite occur in the marble of Verdi Peak in the northern part of the quadrangle. Domain 1 has been penetratingly deformed as indicated by the development of a foliation (S1) and isoclinal folds (F1).

Mesoscopic to macroscopic F2 folds deform the metasedimentary sequence as manifested by folded foliation and compositional layering. A crenulation cleavage (S2) is well-developed in phyllite of the metamorphosed Upper Devonian–Mississippian Pilot Shale. Deformation features of domain 2 include mesoscopic and macroscopic folds and the tilting of the stratigraphic section. Some normal faults cut the sedimentary rocks of domain 2, but not the detachment fault. These normal faults may have developed synchronously with the detachment fault. The Lower Triassic Thaynes Formation and possibly the Permian Park City Group in domain 2 are unconformably overlain by middle Eocene volcanic and volcanoclastic rocks (Tv_s) that predate the development of the southeastern East Humboldt detachment fault. The youngest deformation in the map area

is high-angle normal faulting, which cuts the detachment fault as well as both domains 1 and 2. These normal faults are part of Basin-and-Range normal faulting and are the bounding faults of the eastern flanks of the southeastern East Humboldt Range. The Arizona Spring quadrangle provides the most complete exposure of the stratigraphy and structural features in the upper tier of the East Humboldt Range core complex.

ACKNOWLEDGMENTS

The geologic mapping of the northwestern portion of the Arizona Spring quadrangle was done by Taylor as part of his M.S. thesis (1984) at the University of South Carolina. Subsequent contributions to the completion of this project were provided by Snoke, Howard, Dee, and Thorman. In addition to Snoke (supervisor of the research), Robert D. Hatcher, Jr., Donald T. Secor, Jr., and Pradeep Talwani served on Taylor's M.S. thesis committee. Grant Steele introduced Taylor to the stratigraphy of eastern Nevada during a field trip early in his research studies. We thank Anita G. Harris (U.S. Geological Survey) for her determinations of CAIs in collected conodont-bearing samples from the map area. She also identified conodonts in the Thaynes Formation. We thank Bruce Wardlaw and R. Thomas Lierman (U.S. Geological Survey) for the identification of conodonts in the Gerster Limestone and a CAI determination. We thank Chris Henry for his input and expertise on the volcanic rocks in the map area. Henry found the mapped Eocene ash-flow tuff and limestone units and provided $^{40}\text{Ar}/^{39}\text{Ar}$ dating and lithologic descriptions of the igneous rocks. We thank Andrew Zuza for allowing us to publish a U-Pb zircon age (AZ8-18-22) of a dacite lava and $^{40}\text{Ar}/^{39}\text{Ar}$ ages (H23-W288) of a rhyolite ignimbrite from the map area. Also we greatly appreciate both Phyllis A. Ranz for her expert help on the cartography of the geologic map as well as the preparation of the figures accompanying this report, and Irene Edgerton for her expert help in finalizing the geologic map. The research was funded by the Division of Earth Sciences, National Science Foundation grant EAR8214236 to Snoke.

Taylor thanks Sim and Dee Duval of north Ruby Valley for their hospitality and generosity during the two summers (1982 and 1983) that he lived on their ranch as he did his field work. He thanks Art Snoke for introducing him to the Ruby Mountains–East Humboldt Range metamorphic core complex enigma, and for being a valued mentor during and after the thesis work. He also thanks his wife, Sibby, for her patience, encouragement, and motivation.

Research supported by the U.S. Geological Survey, National Cooperative Geologic Mapping Program, under USGS agreement number G22AC00578. The views and conclusions contained in this document are those of the authors and should not be interpreted as necessarily representing the official policies, either expressed or implied, of the U.S. Government.

REFERENCES

- Brooks, W.E., Thorman, C.H., and Snee, L.W., 1995a, The $^{40}\text{Ar}/^{39}\text{Ar}$ ages and tectonic setting of the middle Eocene northeast Nevada volcanic field: *Journal of Geophysical Research*, v. 100, no. B7, p. 10,403–10,416, <https://doi.org/10.1029/94JB03389>.
- Brooks, W.E., Thorman, C.H., Snee, L.W., Nutt, C.J., Potter, C.J., and Dubiel, R.F., 1995b, Summary of chemical analyses and $^{40}\text{Ar}/^{39}\text{Ar}$ age-spectra data for Eocene volcanic rocks from the central part of the northeast Nevada volcanic field: *U.S. Geological Survey Bulletin* 1988–K, K1–K33.
- Camilleri, P.A., 2010, Geologic map of the Wood Hills, Elko County, Nevada: Nevada Bureau of Mines and Geology Map 172, scale 1:24,000, 16 p.
- Coats, R.R., 1987, Geology of Elko County, Nevada: Nevada Bureau of Mines and Geology Bulletin 101, scale: 1:250,000, 112 p.
- Colgan, J.P., and Henry, C.D., 2009, Rapid Miocene collapse of the Mesozoic orogenic plateau in north-central Nevada: *International Geology Review*, v. 51, p. 920–961, <https://doi.org/10.1080/00206810903056731>.
- Colgan, J.P., Howard, K.A., Fleck, R.J., and Wooden, J.L., 2010, Rapid middle Miocene extension and unroofing of the southern Ruby Mountains, Nevada: *Tectonics*, v. 29, TC6022, <https://doi.org/10.1029/2009TC002655>.
- Collinson, J.W., Kendall, C.G. St. C., and Marcantel, J.B., 1976, Permian-Triassic boundary in eastern Nevada and west central Utah: *Geological Society of America Bulletin*, v. 87, no. 5, p. 821–824.
- Dee, S., and Ressel, M.W., 2016, Preliminary geologic map of the Herder Creek quadrangle, Elko County, Nevada: Nevada Bureau of Mines and Geology Open-File Report 2016-05, scale 1:24,000, 5 p.
- Dee, S.M., Dering, G.M., and Henry, C.D., 2015, Preliminary geologic map of the Heelfly Creek quadrangle and adjacent parts of the Tent Mountain, Soldier Peak, and Secret Valley quadrangles, Elko County, Nevada: Nevada Bureau of Mines and Geology Open-File Report 2015-04, scale 1:24,000, 5 p.
- Henry, C.D., 2008, Ash-flow tuffs and paleovalleys in northeastern Nevada—implications for Eocene paleogeography and extension in the Sevier hinterland, northern Great Basin: *Geosphere*, v. 4, p. 1–35; doi: 10.1130/GES00122.1.
- Henry, C.D., McGrew, A.J., Colgan, J.P., Snoke, A.W., and Brueseke, M.E., 2011, Timing, distribution, amount, and style of Cenozoic extension in the northern Great Basin, in Lee, J., and Evans, J.P., editors, *Geologic field trips to the Basin and Range, Rocky Mountains, Snake River Plain, and terranes of*

- the U.S. Cordillera: Geological Society of America Field Guide 21, p. 27–66, [https://doi.org/10.1130/2011.0021\(02\)](https://doi.org/10.1130/2011.0021(02)).
- Hope, R.A., 1970, Preliminary geologic map of Elko County, Nevada: U.S. Geological Survey Open-File Map, scale: 1:200,000.
- Hope, R.A., 1972, Geologic map of the Spruce Mountain quadrangle, Elko County, Nevada: U.S. Geological Survey Geologic Quadrangle Map GQ-942, scale 1:62,500, 1 sheet, 3 p.
- Hose, R.K., and Repenning, C.A., 1959, Stratigraphy of Pennsylvanian, Permian, and Lower Triassic rocks of the Confusion Range, west-central Utah: American Association of Petroleum Geologists Bulletin, v. 43, p. 2167–2196.
- Hose, R.K., and Blake, M. C., Jr., 1976, Geology and mineral resources of White Pine County, Nevada: Nevada Bureau of Mines and Geology Bulletin 85, p. 1–35.
- Howard, K.A., 1980, Metamorphic infrastructure in the northern Ruby Mountains, Nevada, *in* Crittenden, M.D., Jr., Coney, P.J., and Davis, G.H., editors, Cordilleran metamorphic core complexes; Geological Society of America Memoir 153, p. 335–347, <https://doi.org/10.1130/MEM153-p335>.
- Howard, K.A., 2000, Geologic map of the Lamoille quadrangle, Elko County, Nevada: Nevada Bureau of Mines and Geology Map 125, scale: 1:24,000, 1 sheet, 4 p.
- Howard, K.A., and MacCready, T., 2004, Geologic map of the Verdi Peak quadrangle, Elko County, Nevada: Nevada Bureau of Mines and Geology Map 147, scale: 1:24,000, 1 sheet, 4 p.
- McGrew, A.J., 2018, Geologic map of the Humboldt Peak quadrangle, Elko County, Nevada: Nevada Bureau of Mines and Geology Map 186, scale 1:24,000, 23 p.
- McGrew, A.J., and Snoke, A.W., 2015, Geologic map of the Welcome quadrangle and an adjacent part of the Wells quadrangle, Elko County, Nevada: Nevada Bureau of Mines and Geology Map 184, scale 1:24,000, inset 1:12,000, 40 p.
- Munroe, J.S., and Laabs, B.J., 2013, Temporal correspondence between pluvial lake highstands in the southwestern US and Heinrich Event 1: Journal of Quaternary Science, v. 28, no. 1, p. 49–58.
- Pape, J.R., Sedorff, E., Baril, T.C., and Thompson, T.B., 2016, Structural reconstruction and age of an extensively faulted porphyry molybdenum system at Spruce Mountain, Elko County, Nevada: Geosphere, v. 12, no. 10, p. 237–263, <https://doi.org/10.1130/GES01249.1>.
- Richardson, G.B., 1913, The Paleozoic section in northern Utah: American Journal of Science, v. 36, p. 406–416.
- Sharp, R.P., 1939, Basin-range structure of the Ruby-East Humboldt Range, northeastern Nevada: Geological Society of America Bulletin, v. 50 no. 6, p. 881–920.
- Sicard, K.R., and Snoke, A.W., 2020, Geologic map of the Gordon Creek quadrangle, Elko County, Nevada: Nevada Bureau of Mines and Geology Map 188, scale 1:24,000, 28 p.
- Snelson, S., 1957, The geology of the northern Ruby Mountains and the East Humboldt Range, Elko County, northeastern Nevada: Seattle, University of Washington, Ph.D. dissertation, 214 p.
- Snoke, A.W., 1980, Transition from infrastructure to suprastructure in the northern Ruby Mountains, Nevada, *in* Crittenden, M.D., Jr., Coney, P.J., and Davis, G.H., editors, Cordilleran metamorphic core complexes: Geological Society of America Memoir 153, p. 287–333, <https://doi.org/10.1130/MEM153p287>.
- Snoke, A.W., Howard, K.A., and Dee, S., 2021, Geologic map of the Secret Valley quadrangle, Elko County, Nevada: Nevada Bureau of Mines and Geology Map 189, scale 1:24,000, 21 p.
- Snoke, A.W., Howard, K.A., and Dee, S., 2022, Geologic map of the Soldier Peak quadrangle, Elko County, Nevada: Nevada Bureau of Mines and Geology Map 191, scale 1:24,000, 31 p.
- Snoke, A.W., Howard, K.A., McGrew, A.J., Burton, B.R., Barnes, C.G., Peters, M.T., and Wright, J.E., 1997, The grand tour of the Ruby-East Humboldt metamorphic core complex, northeastern Nevada—part 1—introduction & road log, *in* Link, P.K., and Kowallis, B.J., editors, Proterozoic to recent stratigraphy, tectonics, and volcanology, Utah, Nevada, southern Idaho, and central Mexico: Provo, Utah, Brigham Young University Geology Studies, v. 42, no. 1, p. 225–269.
- Spear, F.S., 1993, Metamorphic phase equilibrium and pressure-temperature-time paths: Washington D.C., Mineralogical Society of America Monograph, 799 p.
- Steele, G., 1960, Pennsylvanian–Permian stratigraphy of east-central Nevada and adjacent Utah: Intermountain Association of Petroleum Geologists Eleventh Annual Field Conference Guidebook, p. 91–113.
- Taylor, G.K., 1984, Stratigraphy, metamorphism, and structure of the southeastern East Humboldt Range, Elko County, Nevada: Columbia, University of South Carolina, M.S. thesis, p. vii + 148.
- Thorman, C.H., 1970, Metamorphosed and nonmetamorphosed Paleozoic rocks in the Wood Hills and Pequop Mountains, northeast Nevada: Geological Society of America Bulletin, v. 81, p. 2417–2448.
- Thorman, C.H., and Brooks, W.E, 1994, Fieldtrip guide to the southern East Humboldt Range, northeast Nevada—age and style of attenuation faults in Permian and Triassic rocks: Nevada Petroleum Society 1994 Fieldtrip Guide, p. 95–99.
- Wardlaw, B.R., and Collinson, J.W., 1978, Stratigraphic relations of Park City Group (Permian) in eastern Nevada and western Utah: The American Association of Petroleum Geologists Bulletin, v. 62, p. 1171–1184.
- Zuza, A.V., Dee, S., Hurlow, H.A., Snoke, A.W., and Laabs, B.J.C., 2021, Preliminary geologic map of the Tent Mountain quadrangle, Elko County, Nevada: Nevada Bureau of Mines and Geology Open-File Report 2021-03, scale 1:24,000, 25 p.

Table 1.

Sample	Map Unit	Latitude NAD83	Longitude NAD83	Lithology	Material	Method	Age (Ma)	$\pm 2\sigma$ (Ma)	K/Ca	$\pm 2s$	n/nt	Reference	Notes
91T22	Eod	40.6424	-115.0920	diorite intrusion	sphene	U-Th-Pb	39.5	0.4				Brooks et al. 1995b	
"	"	"	"	"	"	"	37.8	0.3				Brooks et al. 1995b	
AZ8-18-22 (1)	Eovs	40.70057	-115.07090	dacite lava	zircon	U-Pb	40.1	0.4				This Study	young population
H23-W288	Eot	40.68964	-115.08794	rhyolite ignimbrite	sanidine	$^{40}\text{Ar}/^{39}\text{Ar}$	39.512	0.121	106.7	3.0	12/29	This Study	old population
"	"	"	"	"	sanidine	$^{40}\text{Ar}/^{39}\text{Ar}$	40.076	0.122	71.2	2.1	15/29	This Study	
<div> <div>NAD27</div> <div>NAD27</div> </div>													
91T12	Eovs	40.7031	-115.0728	dacite lava	hornblende	$^{40}\text{Ar}/^{39}\text{Ar}$	39.30	0.80				Brooks et al. 1995 a, b	
91T17	Eovs	40.6678	-115.1061	dacite lava	hornblende	$^{40}\text{Ar}/^{39}\text{Ar}$	40.01	0.60				Brooks et al. 1995 a, b	
91T19	Eovs	40.6967	-115.0789	dacite lava clast in unit Eos	biotite	$^{40}\text{Ar}/^{39}\text{Ar}$	41.51	0.20				Brooks et al. 1995 a, b	

$^{40}\text{Ar}/^{39}\text{Ar}$ dates of Brooks et al. (1995a, b) recalculated to Fish Canyon Tuff sanidine = 28.201 Ma

n/nt = number of grains in calculated age/ total number of grains analyzed. Dates in bold are best estimates of eruption or intrusion age.